

# Rare Semileptonic B Meson Decay In Standard Model

by

Ahzaz Saleem

A thesis  
submitted in partial fulfillment of the  
requirements for the degree of  
Master of Science  
in  
Physics



Supervised by


**Dr. Muhammad Ali Paracha**

School of Natural Sciences(SNS)  
National University of Sciences and Technology  
H-12, Islamabad, Pakistan  
July, 2021

**National University of Sciences & Technology****MS THESIS WORK**


We hereby recommend that the dissertation prepared under our supervision by: Ahzaz Saleem, Regn No. 00000203138 Titled: **Rare Semileptonic B Meson Decay In Standard Model** accepted in partial fulfillment of the requirements for the award of **MS** degree.

**Examination Committee Members**

1. Name: DR. SHAHID IQBAL Signature: 

2. Name: DR. AEYSHA KHALIQUE Signature: 

External Examiner: DR. ISHTIAQ AHMED Signature: 

Supervisor's Name DR. M. ALI PARACHA Signature: 

  
Head of Department

02-07-2021  
Date

**COUNTERSIGNED**

Date: 05/07/2021

  
Dean/Principal

*Dedicated*

*to*

*My Beloved Parents*

# Acknowledgements

I am deeply obliged to ALMIGHTY ALLAH, the most beneficent and merciful. I do obeisance before ALLAH who granted me with the best health and opportunity to be a student of such a passionate and competent teachers. All of this was possible by virtue of Holy Prophet MUHAMMAD (S.A.W), whose principles enlighten us at every stage of life.

I would like to take the opportunity to pay my deepest gratitude to my supervisor **Dr. Muhammad Ali Paracha**, Associate Professor, SNS, NUST, Islamabad Pakistan, for his commitment, guidance encouragement and valuable suggestions during the course of this journey. I would like to thank my Guidance and Examination Committee (GEC) members, **Dr. Shahid Iqbal** and **Dr. Ayesha Khaliq**, for their kind support, encouragement and insightful comments. I am extremely gratified to them who believed in my efforts. May Allah showers his countless blessing upon them and bless them with good health and knowledge. I also thanks to, **Dr. Saadi Ishaq**, for their encouragement, and valuable suggestions.

I am also pleased to all the SNS faculty members and administration for their support.

A special and sincere feelings of gratitude to my loving parents specially my late mother, sibilings and all other family members whose love and prayers have always been a source of strength for me. I am also thankful to all my friends especially Talha Haroon Khan, Younas Khan, Hamza Haroon khan, M Ismail Khan, Khizar Ayaz, Bilal Khan, Syed Nouman Shah and all others.

**Ahzaz Saleem**

# Abstract

The semileptonic  $B \rightarrow K_1(1270, 1400)\mu^+\mu^-$  decay has been analyzed in the framework of the Standard Model. The final state meson  $K_1(1270)$  and  $K_1(1400)$  are the mixtures of the  $K_{1A}$  and  $K_{1B}$ , which are the  $^1P_1$  and  $^3P_1$  state with mixing angle  $\theta_{K_1}$ . In this regard, various observables such as branching ratio  $\mathcal{BR}$ , forward-backward asymmetry  $\mathcal{A}_{FB}$ , Longitudinal helicity Fraction  $f_L$  and ratio of final state meson  $K_1(1400)$  to  $K_1(1270)$ ,  $R_\mu(K_1) = \mathcal{B}(B \rightarrow K_1(1400)\mu^+\mu^-) / \mathcal{B}(B \rightarrow K_1(1270)\mu^+\mu^-)$  have been investigated. To investigate the said observables we have used light cone QCD sum rules and the values of mixing angle are  $\theta_K = -34^\circ, -45^\circ, -57^\circ$ . It is found that the physical observables under consideration are sensitive to the mixing angle  $\theta_{K_1}$  for the decay  $B \rightarrow K_1(1400)\mu^+\mu^-$  and almost insensitive for the decay  $B \rightarrow K_1(1270)\mu^+\mu^-$ . It is also found that the said decays are sensitive to the ratio  $R_\mu(K_1)$ . Hence the ratio  $R_\mu(K_1)$  is useful to determine  $\theta_{K_1}$  and complement for other observables to test SM parameters and to probe the structure of NP.

# Contents

<b>List of Figures</b>	<b>vii</b>
<b>List of Tables</b>	<b>ix</b>
<b>1 Introduction</b>	<b>1</b>
<b>2 Standard Model</b>	<b>6</b>
2.1 Gauge Principle . . . . .	6
2.2 Lagrangian for standard model . . . . .	7
2.2.1 Gauge Symmetric Group . . . . .	8
2.2.2 fermionic part . . . . .	9
2.2.3 Higgs Lagrangian . . . . .	10
2.2.4 Higgs Mechanism . . . . .	11
2.2.5 Fermion masses, $\mathcal{L}_{Yukawa}$ . . . . .	13
<b>3 Theoretical Formalism For Flavor And B Mesons Physics</b>	<b>16</b>
3.1 Cabibbo Kobayashi Maskawa (CKM) matrix . . . . .	16
3.1.1 Standard Parametrization . . . . .	17
3.1.2 Wolfenstein Parametrization . . . . .	18
3.2 Weak Decays of Hadrons . . . . .	18
3.2.1 Effective Field Theory . . . . .	19
3.2.2 Operator Product Expansion . . . . .	20

3.2.3	Effective Hamiltonian . . . . .	21
3.2.4	Weak Decays of B Mesons . . . . .	23
3.2.5	Rare B mesons decay . . . . .	24
3.3	Flavour Changing Neutral Currents . . . . .	25
3.3.1	GIM Mechanism . . . . .	26
3.4	Decay Amplitude for Hadronic Decays . . . . .	27
3.4.1	Amplitude for Rare B decay at Quark Level . . . . .	27
<b>4</b>	<b>The Decay <math>B \rightarrow K_1(1270, 1400)\mu^+\mu^-</math> in the Standard Model</b>	<b>29</b>
4.1	Ingredients for $B \rightarrow K_1\mu^+\mu^-$ . . . . .	29
4.2	Form Factor And Mixing of <b><math>K_1(1270) - K_1(1400)</math></b> . . . . .	30
4.3	Helicity Amplitudes . . . . .	35
4.4	Physical Observables . . . . .	36
4.4.1	Differential Decay Rate ( $\frac{d\Gamma}{dq^2}$ ) . . . . .	36
4.4.2	Forward Backward Asymmetry . . . . .	37
4.4.3	Longitudinal Helicity Fraction . . . . .	39
4.4.4	<b><math>K_1(1400)</math> to <math>K_1(1270)</math> Ratio, (<math>R_\mu(K_1)</math>)</b> . . . . .	40
<b>5</b>	<b>Conclusion</b>	<b>45</b>
	<b>Appendix</b>	<b>46</b>
	<b>Appendix</b>	<b>54</b>

# List of Figures

3.1	$c \rightarrow s\bar{u}d$ in full and effective theory . . . . .	20
3.2	Change of flavour with the exchange of W boson. . . . .	25
	(a) Loop diagram of $\bar{b}$ to $s$ decay . . . . .	25
	(b) Loop diagram of $b$ to $s$ decay . . . . .	25
3.3	Change of flavour with the exchange of W boson. . . . .	26
	(a) penguin diagram . . . . .	26
3.4	Electroweak Loop or penguin diagram for $b \rightarrow sl^+l^-$ in SM dominant contributions. . . . .	27
4.1	Branching ratio for the decay $B \rightarrow K_{1(1270)}\mu^+\mu^-$ and $B \rightarrow K_{1(1400)}\mu^+\mu^-$ in Standard Model. The green, red and blue curves belongs to angles $\theta_{K_1} = -34^\circ, -45^\circ, -57^\circ$ with positive and negative uncertainties in the form factor. . . . .	37
4.2	Forward-Backward Asymmetry for $B \rightarrow K_{1(1270)}\mu^+\mu^-$ and $B \rightarrow K_{1(1400)}\mu^+\mu^-$ . The green, red and blue curves belongs to angles $\theta_{K_1} = -34^\circ, -45^\circ, -57^\circ$ with positive and negative uncertainties in the form factor. . . . .	38
4.3	longitudnal Helicity Amplitude for the decay $B \rightarrow K_{1(1270)}\mu^+\mu^-$ and $B \rightarrow K_{1(1400)}\mu^+\mu^-$ . The green, red and blue curves belongs to angles $\theta_{K_1} = -34^\circ, -45^\circ, -57^\circ$ with positive and negative uncertainties in the form factor. . . . .	39



- 4.4 The  $R_\mu(K_1) = \mathcal{B}(B \rightarrow K_1(1400)\mu^+\mu^-) / \mathcal{B}(B \rightarrow K_1(1270)\mu^+\mu^-)$  with longitudinal  $R_\mu^L(K_1)$  and transverse  $R_\mu^T(K_1)$  ratio, as a function of  $\theta_{K_1}$ . The green, red and blue curves belongs to angles  $\theta_{K_1} = -34^\circ, -45^\circ, -57^\circ$  with positive and negative uncertainties in the form factor. . . . . 41

# List of Tables

2.1	.....	10
4.1	Form Factor [60] for $B \rightarrow K_{1A,1B}$ , here $x$ and $y$ are the parameter of the form factor. ....	32
4.2	Wilson Coefficients $C_i^\mu$ in th Standard Model at the scale $\mu \sim m_b$ . . . .	33
4.3	Input parameters for numerical calculations [59, 62, 65]. . . . .	42
4.4	Branching ratio $\mathcal{BR}$ for $B \rightarrow K_1(1270)\mu^+\mu^-$ at different angle in SM with negative and positive uncertainties in the form factors. . . . .	42
4.5	Branching ratio $\mathcal{BR}$ for $B \rightarrow K_1(1400)\mu^+\mu^-$ at different angle in SM with negative and positive uncertainties in the form factors. . . . .	42
4.6	Branching ratio for $B \rightarrow K_1(1270)\mu^+\mu^-$ and $B \rightarrow K_1(1400)\mu^+\mu^-$ in different bin of $q^2$ . . . . .	43
4.7	Forward-backward symmetry for $B \rightarrow K_1(1270)\mu^+\mu^-$ and $B \rightarrow K_1(1400)\mu^+\mu^-$ in different bin of $q^2$ . . . . .	43
4.8	Helicity fraction for $B \rightarrow K_1(1270)\mu^+\mu^-$ and $B \rightarrow K_1(1400)\mu^+\mu^-$ in different bin of $q^2$ . . . . .	43
4.9	Ratio $R_\mu(K_1) = \mathcal{B}(B \rightarrow K_1(1400)\mu^+\mu^-)/(\mathcal{B}B \rightarrow K_1(1270)\mu^+\mu^-)$ in different bin of $q^2$ . . . . .	44

# Chapter 1

## Introduction

The Standard model (SM) of particle physics [1, 2, 3] is a theory describing three fundamental forces, the strong nuclear force, weak nuclear force and electromagnetic force. Though SM is successful theory, as it is consistent with current experimental data with great precision.

Despite its many successes, it has some theoretical limitations which hinder its status as a fundamental theory. These limitations are as follows:

- In SM the Neutrinos are massless but the experiments have shown that neutrinos have mass.
- Why the gravity is not incorporated?
- Why is the electroweak scale so small (hierarchy problem)?
- What is the origin of the mass patterns among the fermions?
- Why only the three generations of quarks and leptons?

These limitations indicate that there is physics beyond the SM. In literature many physics beyond the SM has been studied such as 2HDM, ExtraLIM Model, leptoquark Models, Z' Models and many more.

In this thesis we work extensively in the framework of SM, particularly in the flavor sector.

In flavor physics the ideal laboratory system is B meson, which impart a window pane to investigate the physics in the SM as well as beyond the SM.

B-physics started in 1977 with the result of a dimuon resonance at 9.5 GeV in 400 GeV proton-nucleon collision at Fermilab [4] and was named  $\Upsilon$  resonances, its quark content is  $\bar{b}b$ . The dedicated B-factories Babar [5] and Belle [6] started working in 1999 and added a large amount of data to the results of CLEO [7], CERN [8] and Fermilab experiments [9]. The recent experiment such as Large Hadron collider (LHC) will not only offer a good testing ground to study the SM with great precision but also to investigate the new physics (NP) effects through the deviations of measured observables from SM values.

In SM the interactions of quarks flavor involves the conversion of certain flavors from one flavor to another. In the SM the flavor symmetry is exact at tree level and its violation at loop level is very small. Such processes in the flavor sector are rare B-meson decays. Rare B decays are mediated through flavor changing neutral current transitions (FCNC), which are induced only at loop level through Glashow-Iliopoulos-Maiani (GIM) mechanism [10] in the SM. These FCNC transitions are a suitable tool to study the physics within and beyond the SM. Furthermore in SM these are also suppressed because of their dependence on the weak mixing angles of the quark-flavor rotation matrix the Cabibbo-Kobayashi-Maskawa (CKM) matrix. These two conditions make the FCNC decays relatively rare.

The experimental examination of the inclusive and exclusive decay  $B \rightarrow K^* \gamma$  and  $B \rightarrow X_s \gamma$  has promoted a great theoretical interest in rare B meson decays [11, 12]. The inclusive decays are theoretically better understood but are challenging to study experimentally. In contrast, the exclusive decays are easier to discover experimentally but difficult to calculate theoretically; and the difficulty lies in describing the hadronic structure, which involves non-perturbative physics and provides the main uncertainty in the predictions of exclusive rare decays. In case of exclusive decays any reliable extraction of the short distance effects are encrypted in Wilson coefficients of the effective Hamiltonian provide a precise separation of the long distance contributions [13, 14], that should be known with high accuracy. The long-distance effects in the meson

transition amplitude of the effective Hamiltonian are encoded in the meson transition form factors which are the functions of square of momentum transfer and are model dependent quantities.

The exclusive rare semileptonic and rare radiative decays of B meson such as  $B \rightarrow \gamma l^+ l^-$  [15, 16],  $B \rightarrow K(K^*) l^+ l^-$  [17, 18, 19, 20, 21, 22, 23] and  $B \rightarrow \phi l^+ l^-$  [24] decays based upon  $b \rightarrow s(d) l^+ l^-$  have been studied in literature using the frameworks of constituent quark model, Light cone QCD sum rules to express the meson transition form factors. Out of these the exclusive semileptonic decay  $B \rightarrow K^* l^+ l^-$  that governed by the quark-level transition  $b \rightarrow s l^+ l^-$  is one of the most interesting processes, which has got a great attention, experimentally as well as theoretically [25]. The exploration of physics within the SM through various inclusive B meson decays like  $B \rightarrow X_{s,d} l^+ l^-$  and their corresponding exclusive processes,  $B \rightarrow M l^+ l^-$  with  $M = K, K^*, K_1, \rho$  etc have been completely set on phenomenology in literature by the numerical values of Wilson coefficients of only three operators evaluated at the scale  $\mu \sim m_b$ . These studies showed that the above mentioned inclusive and exclusive decays of B meson are very sensitive to the flavor structure of the SM and impart a raindrop for any NP model. The FCNC decay modes like  $B \rightarrow X_s l^+ l^-$ ,  $B \rightarrow K^* l^+ l^-$  and  $B \rightarrow K l^+ l^-$  in particular involved observables which can distinguish between the various extensions of the SM. The combined charged and neutral B meson Branching Ratio ( $\mathcal{BR}$ ) for  $B \rightarrow K \mu^+ \mu^-$  by Belle [26] is given as,

$$\mathcal{B}(B \rightarrow K \mu^+ \mu^-) = 0.99_{-0.32-0.14}^{+0.40+0.13} \times 10^{-6}$$

The observables like branching ratio ( $\mathcal{BR}$ ), forward-backward asymmetry ( $\mathcal{A}_{FB}$ ) and helicity fractions ( $f$ ) of final state mesons for the semileptonic B decays are greatly influenced within and beyond the SM. Therefore, the precise measurement of these observables will play an important role in the precision of SM. The purpose of this thesis is to investigate the possibility of  $B \rightarrow K_1(1270, 1400) l^+ l^-$  in the SM at different mixing angle  $\theta_{K_1}$  using the above mentioned physical observables. The study of these physical observables will provide a precision test of SM and NP when more

data will be available at LHC.

The Observables that mentioned as above have been studied extensively for quark level decays  $b \rightarrow s(d)l^+l^-$ . The  $K_1$  meson in  $B$  decays has been observed in  $B \rightarrow J/\psi K_1$ ,  $B \rightarrow K_1 \gamma$ , and  $B \rightarrow K_1 \phi$  transition channels [27]. After Belle [28] has announced the first measurement of  $B \rightarrow K_1^+(1270)\gamma$ ,

$$\mathcal{B}(B^+ \rightarrow K_1^+ \gamma) = (4.28 \pm 0.94 \pm 0.43) \times 10^{-5},$$

these radiative decays become a topic of supreme interest and we saw great theoretical progress in this regard. Like the  $B \rightarrow K^*(892)l^+l^-$  [29], the studied has been made of semileptonic B meson decay  $B \rightarrow K_1 l^+ l^-$  with  $K_1$  an axial vector meson. The axial vector meson and vector meson is distinguished by the Dirac gamma structure of decay amplitude ( $\gamma_5$ ) and some non perturbative parameters. In this context, our said decay  $B \rightarrow K_1(1270, 1400)\mu^+\mu^-$  is productive in phenomenology as the physical states  $K_1(1270)$  and  $K_1(1400)$  are mixture of  $^3P_1$  and  $^1P_1$  states  $K_{1A}$  and  $K_{1B}$  which is obtain as,

$$\begin{aligned} |K_1(1270)\rangle &= |K_{1A}\rangle \sin \theta_{K_1} + |K_{1B}\rangle \cos \theta_{K_1} \\ |K_1(1400)\rangle &= |K_{1A}\rangle \cos \theta_{K_1} - |K_{1B}\rangle \sin \theta_{K_1} \end{aligned}$$

In this thesis we will study the physical observables like branching ratio ( $\mathcal{BR}$ ), forward-backward asymmetry ( $\mathcal{A}_{FB}$ ) and longitudinal helicity fractions ( $f_L$ ) and branching fractions  $R_\mu(K_1) = \mathcal{B}(B \rightarrow K_1(1400)\mu^+\mu^-) / \mathcal{B}(B \rightarrow K_1(1270)\mu^+\mu^-)$  of final state meson  $K_1(1270)$  and  $K_1(1400)$  at different angle  $\theta_K = -34^\circ, -45^\circ, -57^\circ$ . To study these observables, we have used the Light Cone QCD sum rules form factors. It is observed that the  $\mathcal{BR}$  is suppressed for  $K_1(1400)$  as a final state meson compared to that of  $K_1(1270)$ . The magnitude of the mixing angle  $\theta_{K_1}$  has been approximated to be  $-34^\circ \leq \theta_{K_1} \leq -57^\circ$  [30]. Previously from the study of  $\tau \rightarrow K_1(1270)\nu_\tau$  and  $B \rightarrow K_1(1270)\gamma$  the  $\theta_{K_1}$  has been set to be  $\theta_{K_1} = -(34 \pm 13)^\circ$ , where minus sign related to the selected phase of  $|K_{1A}\rangle$  and  $|K_{1B}\rangle$  [32].

This thesis is organize as :

In chapter 2 we will study flavor picture as well as some basics of SM particles and their interactions such as the masses and coupling constants. This will help us to understand the flavor picture of SM.

In chapter 3 we will focus on the theoretical framework and tools that deal with flavor physics. In the first section (3.1) we will briefly discuss the quark mixing matrix the Cabibbo-Kobayashi-Maskawa (CKM) matrix. Then we will discuss about weak decays of hadrons in which we will write the Effective Hamiltonian that is the basic ingredient of the effective theory and also for our considered process. In next section we will put focus on general picture of the amplitude for the decays with the help of Effective Hamiltonian, that will lead to understand the semileptonic B Meson transition from  $B \rightarrow K_1 l^+ l^-$ .

In chapter 4 we will study the exclusive  $B \rightarrow K_1(1270, 1400) \mu^+ \mu^-$  process that at quark level is given as  $b \rightarrow s \mu^+ \mu^-$ , firstly we will write the effective hamiltonian to express the amplitude in term of helicity, then we will put some focus on form factors and mixing of the  $K_1(1270)$  and  $K_1(1400)$  and at the end of chapter we will discuss the different observables like  $\mathcal{BR}$ ,  $\mathcal{A}_{FB}$  and longitudinal helicity fractions ( $f_L$ ) and will study their behaviour through graphs.

Finally we have to sum up our discussion with conclusion.

# Chapter 2

## Standard Model

The Standard Model (SM) of particle physics [1, 2, 3] comprises with the strong, weak, and electromagnetic interactions that are based upon the gauge symmetry  $SU(3)_C \times SU(2)_L \times U(1)_Y$  leaving the gravitational force yet. The SM corresponds to a non-abelian gauge principle. A gauge theory is a quantum field theory (QFT) that is based upon the principle of the local gauge invariance or the gauge principle [33, 34, 35].

### 2.1 Gauge Principle

The gauge principle give a process to transform Lagrangian, which is invariant according to transformation of global symmetry of some non-abelian symmetry group  $SU(N)$  into Lagrangian, which is therefore invariant according to local symmetry transformation or gauge invariant. Let Lagrangian  $\mathcal{L}(\Phi, \partial_\mu \Phi)$  is invariant under  $SU(N)$  global symmetry transformation.

$$\Phi(x) \rightarrow O\Phi(x) \quad : \quad O^{-1} = O^\dagger \quad (2.1)$$

Our motivation is to built a theory which is also invariant according to local  $SU(N)$  transformation.

$$\Phi(x) \rightarrow e^{i\alpha^a(x)X^a}\Phi(x) \quad : \quad O(x) = e^{i\alpha^a(x)X^a} \quad (2.2)$$

The issue arises when the Lagrangian is no more locally invariance. In order to restore the invariance in Lagrangian, one has to replace  $\partial_\mu$  with a covariant derivative  $\mathcal{D}_\mu$  that



will transform like a field.

$$\mathcal{D}_\mu = \partial_\mu - ig\hat{\mathcal{A}}_\mu \quad : \quad \hat{\mathcal{A}}_\mu = X^a \mathcal{A}_\mu^a \quad (2.3)$$

$\mathcal{D}_\mu$  transform as

$$\mathcal{D}_\mu \Phi(x) \rightarrow (\mathcal{D}_\mu \Phi(x))' = O(x)(\mathcal{D}_\mu \Phi(x)) \quad (2.4)$$

$g$  is term as coupling constant,  $\mathcal{A}_\mu^a$  is used for the set of gauge field and  $X^i$  is generator of symmetry group and follows the algebra as

$$[X^a, X^b] = if^{abc}X^c \quad (2.5)$$

$f^{abc}$  is structure constant. The transformation of  $\mathcal{A}$  in order to prevent the gauge invariance is like

$$\mathcal{A}_\mu^a \rightarrow \mathcal{A}_\mu^{a'} = O(x)\left(\frac{i}{g}\partial_\mu + \mathcal{A}_\mu^a\right)O^\dagger(x) \quad (2.6)$$

Ultimately by adding the kinetic term for gauge field: locally invariant term which rely on  $\mathcal{A}_\mu$  and its derivative, but not on  $\Phi$ , the field strength tensor  $F_{\mu\nu}$ , look like.

$$F_{\mu\nu}^a = \partial_\mu \mathcal{A}_\nu^a - \partial_\nu \mathcal{A}_\mu^a - gf^{abc} \mathcal{A}_\mu^b \mathcal{A}_\nu^c \quad (2.7)$$

Now we will get the kinetic term which will be locally invariant by multiplying  $F_{\mu\nu}$  with  $F^{\mu\nu}$  and emerge in Lagrangian. the new  $\mathcal{L}$  will read as locally invariant.

$$\mathcal{L} = \mathcal{L}(\Phi, \mathcal{D}_\mu \Phi) - \frac{1}{4}F_{\mu\nu}F^{\mu\nu} \quad (2.8)$$

We can extract the information regarding gauge field interactions by gauge principle that stretched out a global to local symmetry.

## 2.2 Lagrangian for standard model

The general picture of the SM Lagrangian [3] is given as .

$$\mathcal{L}_{SM} = \mathcal{L}_{gauge} + \mathcal{L}_{fermion} + \mathcal{L}_{yukawa} + \mathcal{L}_{higgs} \quad (2.9)$$

$\mathcal{L}_{gauge}$  defines the gauge symmetric group  $SU(3)_C \times SU(2)_L \times U(1)_Y$ ,  $\mathcal{L}_{fermion}$  is the fermions sector,  $\mathcal{L}_{Yukawa}$  presents the yukawa interactions and  $\mathcal{L}_{higgs}$  is the higgs sector.

### 2.2.1 Gauge Symmetric Group

The field that arise from the gauge symmetries are called gauge field, the gauge part carry twelve gauge fields depending on the gauge group dimensions. The gauge group  $SU(3)_C$  predicts the field that give rise the strong force QCD (Quantum Chromodynamics) with the exchange of gauge bosons are gluons.  $SU(2)_L \times U(1)_Y$  gauge group corresponds to the Glashow Weinberg Salam theory of electroweak interactions. The corresponding particles to  $SU(2)_L$  are  $W^\pm$  and Z gauge boson in the SM. These particles are the vector bosons that act as the weak force carrier.  $U(1)_Y$  is a unitary group deal with the electromagnetic force between the particles with the exchange of photon. The right handed neutrino are neutral according to three gauge groups so they would not added. The Lagrangian for gauge field section will look like.

$$\mathcal{L}_{gauge} = -\frac{1}{4}G_{\mu\nu}^i G_i^{\mu\nu} - \frac{1}{4}W_{\mu\nu}^i W_i^{\mu\nu} - \frac{1}{4}B_{\mu\nu} B^{\mu\nu} \quad (2.10)$$

Where  $B_{\mu\nu}$ ,  $W_{\mu\nu}^i$  and  $G_{\mu\nu}^i$  are field strength tensor of electromagnetic, weak and strong forces respectively, which are given as,

$$\begin{aligned} U(1)_Y &\rightarrow B_{\mu\nu} = \partial_\mu B_\nu - \partial_\nu B_\mu \\ SU(2)_L &\rightarrow W_{\mu\nu}^i = \partial_\mu W_\nu^i - \partial_\nu W_\mu^i + g' \epsilon^{ijk} W_\mu^j W_\nu^k \\ SU(3)_C &\rightarrow G_{\mu\nu}^i = \partial_\mu G_\nu^i - \partial_\nu G_\mu^i + g_s f^{ijk} G_\mu^j G_\nu^k \end{aligned} \quad (2.11)$$

The corresponding covariant derivatives  $\mathcal{D}_\mu$  is given as,

$$\begin{aligned} \mathcal{D}_\mu &= \partial_\mu - ig_e Y B_\mu \\ \mathcal{D}_\mu &= \partial_\mu - ig' \frac{\sigma^i}{2} W_\mu^i \\ \mathcal{D}_\mu &= \partial_\mu - ig_s \frac{\tau^i}{2} G_\mu^i \end{aligned} \quad (2.12)$$

In Eq.(2.11)  $G_\mu^i$  is associated with the  $SU(3)_C$  color symmetry group where  $i=1,2,\dots,8$  shows the number of gluons.  $W_\mu^i$  related to the  $SU(2)_L$  weak isospin here  $i=1,2,3$  tells us about the three gauge boson and  $B_\mu$  associated with the  $U(1)_Y$  weak hypercharge.  $\epsilon^{ijk}$  and  $f^{ijk}$  are the structure constant,  $g$  is the coupling constant which runs with the energy scales, as  $g_e$ ,  $g'$  and  $g_s$  are the coupling constants for electromagnetic interaction, weak-isospin and strong interactions, respectively. The non abelian gluon field

strength tensor  $G_{\mu\nu}^i$  and field strength tensor for weak iso-spin  $W_{\mu\nu}^i$  have the extra term which pointed toward the field self interaction in opposite of abelian electromagnetic field tensor  $B_{\mu\nu}$ . So the main difference between the non abelian and abelian field strength tensor is the extra term that leads to the field self interaction in non abelian field strength tensor and implies the asymptotic freedom in QCD.

### 2.2.2 fermionic part

Fermion set in three generations in standard model and each generation consist of up(u) and down(d) type quark, charged lepton and corresponding neutrino. These are further classified into right handed and left handed fermions which are siglets and doublets respectively, with respect to  $SU(2)_L$  which are given as below.

$$\begin{aligned} L_L^i &= \begin{pmatrix} \nu_{eL} \\ e_L \end{pmatrix}, \quad \begin{pmatrix} \nu_{\mu L} \\ \mu_L \end{pmatrix}, \quad \begin{pmatrix} \nu_{\tau L} \\ \tau_L \end{pmatrix} \\ q_L^i &= \begin{pmatrix} u_L \\ d_L \end{pmatrix}, \quad \begin{pmatrix} c_L \\ s_L \end{pmatrix}, \quad \begin{pmatrix} t_L \\ b_L \end{pmatrix} \end{aligned} \quad (2.13)$$

now the siglets are as fallow

$$\begin{aligned} e_R^i &= (e_R, \mu_R, \tau_R) \\ u_R^i &= (u_R, c_R, t_R) \\ d_R^i &= (d_R, s_R, b_R) \end{aligned} \quad (2.14)$$

In term of quarks and lepton field, the fermionic part of lagrangian can be expressed as,

$$\mathcal{L}_{fermion} = i\bar{L}_L^i \not{D}_L L_L^i + i\bar{q}_L^i \not{D}_q q_L^i + i\bar{e}_R^i \not{D}_e e_R^i + i\bar{u}_R^i \not{D}_u u_R^i + i\bar{d}_R^i \not{D}_d d_R^i \quad (2.15)$$

By defination  $\not{D} = \gamma_\mu D^\mu$  is a covariant derivative which explicitly acting on the fermion fields given as,

$$\begin{aligned} D_{L_L}^\mu &= \partial_\mu - ig_e Y_L B^\mu - ig' \frac{\sigma^i}{2} W^{i,\mu}, \\ D_{q_L}^\mu &= \partial_\mu - ig_e Y_q B^\mu - ig' \frac{\sigma^i}{2} W^{i,\mu} - ig_s \tau^i G^{i,\mu}, \\ D_{e_R}^\mu &= \partial_\mu - ig_e Y_e B^\mu, \\ D_{a_R}^\mu &= \partial_\mu - ig_e Y_a B^\mu - ig_s \tau^i G^{i,\mu}, \quad a = u, d \end{aligned} \quad (2.16)$$

$\sigma^i$  represents the Pauli matrices the generator of  $SU(2)$ ,  $Y$  is hypercharge and  $\tau^i$  used as the  $SU(3)_C$  generators and associated to Gell Mann matrixes as  $\tau^i = \frac{\lambda^i}{2}$ .

**Table 2.1**

Spinor Field	Colour	Weak Iso-spin	Hypercharge
$q_L^i$	3	2	$Y_q = +1/3$
$u_R^i$	3	1	$Y_u = +4/3$
$d_R^i$	3	1	$Y_d = +1/3$
$L_L^i$	1	2	$Y_L = -1$
$e_R^i$	1	1	$Y_e = -2$

The weak interaction only subsist on lepton doublet and left quark in agreement to weak interctions theory.

$$\begin{aligned} \mathcal{L}_{fermion} &= i(\bar{u}_L, \bar{d}_L)\gamma_\mu(\partial_\mu - ig\left(\frac{\sigma^i}{2}\right)W_\mu^i) \begin{pmatrix} u_L \\ d_L \end{pmatrix} \\ &= i\bar{u}_L\gamma_\mu\partial_\mu u_L + i\bar{d}_L\gamma_\mu\partial_\mu d_L - \frac{1}{2}g\bar{u}_L\gamma_\mu W_\mu^- d_L - \frac{1}{2}g\bar{d}_L\gamma_\mu W_\mu^+ u_L \end{aligned} \quad (2.17)$$

The flavor changing of quarks from up to down and down to up is take place with the exchange of  $W^\pm$  gauge boson. This type of interaction is term as change curent.

$$\mathcal{L}_{cc} = -\frac{1}{2}g\bar{u}_L\gamma_\mu W_\mu^- d_L - \frac{1}{2}g\bar{d}_L\gamma_\mu W_\mu^+ u_L \quad (2.18)$$

Till now all the gauge bosons, quarks and leptons are massless. In the next section we will discuss the Higgs Mechanism which is responsible to give masses to these particles

### 2.2.3 Higgs Lagrangian

The higgs part of SM Lagrangian may introduce by additional complex scalar field in an existing theory which has a hypercharge  $Y_\phi = \frac{1}{2}$  and doublet as for  $SU(2)_L$ .

$$\phi = \begin{pmatrix} \phi_+ \\ \phi_0 \end{pmatrix} = \frac{1}{\sqrt{2}} \begin{pmatrix} \phi_1 + i\phi_2 \\ \phi_3 + i\phi_4 \end{pmatrix} \quad (2.19)$$

The extra term is set in the SM Lagrangian as

$$\mathcal{L}_{Higgs} = (\mathcal{D}^\mu \phi)^\dagger (\mathcal{D}_\mu \phi) - V(\phi) \quad (2.20)$$

The covariant derivative  $\mathcal{D}_\mu$  and potential  $V(\phi)$  is given as

$$\begin{aligned}\mathcal{D}_\mu &= \partial_\mu - \frac{1}{2}ig_e B_\mu - \frac{1}{2}ig' \sigma^i W_\mu^i \\ V(\phi) &= m^2 \phi^\dagger \phi - \lambda(\phi^\dagger \phi)^2\end{aligned}\tag{2.21}$$

By using these values the Higgs Lagrangian will look like as

$$\mathcal{L}_{Higgs} = |\partial_\mu - \frac{1}{2}ig_e B_\mu - \frac{1}{2}ig' \sigma^i W_\mu^i|^2 |\phi|^2 - \frac{m^2}{2} |\phi|^2 - \frac{\lambda}{4} |\phi|^4\tag{2.22}$$

## 2.2.4 Higgs Mechanism

In SM the gauge invariance does not allow the mass terms in Lagrangian for chiral fermions and gauge bosons. However, experimently it is well known that all fermions and weak guage boson acquires mass. In SM mostly the particles can get masses via spontaneous symmetry break (SSB) known as Higgs Mechanism. In Higgs Mechanism a complex scalar doublet is added to the SM Lagrangian.

$$\mathcal{L}_{Higgs} = (\mathcal{D}^\mu \phi)^\dagger (\mathcal{D}_\mu \phi) - m^2 \phi^\dagger \phi - \lambda(\phi^\dagger \phi)^2\tag{2.23}$$

Where is  $V(\phi)$  in above eqn, clearly write it down. The  $V(\phi)$  is the Higgs potential which steers the SSB.  $\lambda$  is quartic coupling defines the self interaction between the scalar field. For vacuum stability  $\lambda > 0$  and  $\mu^2 > 0$  then the potential ( $\phi$ ) acquire the vacuum expectation value (VEV) and in result the symmetry will break spontaneously. Because of symmetry of potential we have infinite number of degenerate states with least energy assuring the equation

$$\phi^\dagger \phi = \frac{\mathcal{V}^2}{2} \quad , \quad \mathcal{V}^2 = \frac{m^2}{\lambda}.\tag{2.24}$$

Using these transformation and introduce the real  $h$  field as  $\phi = \frac{1}{\sqrt{2}}(\mathcal{V} + h)$  in Lagrangian Eq.(2.22), that will expression as

$$\begin{aligned}\mathcal{L} &= (\partial_\mu + ig\mathcal{A}_\mu) \frac{1}{\sqrt{2}}(\mathcal{V} + h) (\partial_\mu - ig\mathcal{A}_\mu) \frac{1}{\sqrt{2}}(\mathcal{V} + h) - \frac{1}{2}m^2(\mathcal{V} + h)^2 - \frac{1}{4}\lambda(\mathcal{V} + h)^4 \\ &= \frac{1}{2}(\partial_\mu h)^2 + \frac{1}{2}g^2 \mathcal{A}_\mu^2 (\mathcal{V} + h)^2 - \lambda \mathcal{V}^2 h^2 - \lambda \mathcal{V} h^3 - \frac{1}{4}\lambda h^4 + \frac{1}{4}\lambda \mathcal{V}^4 \\ &= \frac{1}{2}(\partial_\mu h)^2 - \lambda \mathcal{V}^2 \mathcal{A}_\mu^2 + \frac{1}{2}g^2 \mathcal{V}^2 \mathcal{A}_\mu^2 + g^2 \mathcal{V} \mathcal{A}_\mu^2 h + \frac{1}{2}g^2 \mathcal{A}_\mu^2 h^2 - \lambda \mathcal{V} h^3 - \frac{1}{4}\lambda h^4\end{aligned}\tag{2.25}$$

The  $\mathcal{L}$  is even now invariant under the  $SU(2)_L \times U(1)_Y$  symmetry, however ground state is not,  $\mathcal{A}^2 h$ ,  $\mathcal{A}^2 h^2$ ,  $h^3$  and  $h^4$  are the interacting terms in eq.(2.28). That is, electromagnetism is unbreakable by scalar VEV. Thus VEV yields the breaking scheme as,

$$SU(2)_L \times U(1)_Y \rightarrow U(1)_Q \quad (2.26)$$

which is even now a true vacuum symmetry. The so called Goldstone bosons is taken out by  $\mathcal{A}_\mu$  gauge boson and provides it a mass.

### Guage Boson Massess

We have observed that any choice of vacuum that can breaks a symmetry will generate a mass for the corresponding gauge boson. For convenience the scalar doublet in the unitary guage is written as fallow

$$\phi = \begin{pmatrix} \phi_+ \\ \phi_0 \end{pmatrix} = \frac{1}{\sqrt{2}} \begin{pmatrix} 0 \\ \mathcal{V} + h \end{pmatrix} \quad (2.27)$$

We are intended only in the contribution of the gauge boson masses this is how we leave any  $h$  mixed term. The gauge boson mass terms derive from the kinetic term of the Higgs Lagrangian, the part that evaluate the gauge boson masses are

$$\begin{aligned} (D^\mu \phi)^\dagger (D_\mu \phi) &= \left| \left( \partial_\mu - \frac{i}{2} g_e B_\mu - i \frac{\sigma^i}{2} g' W_\mu^i \right) \frac{1}{\sqrt{2}} \begin{pmatrix} 0 \\ \mathcal{V} \end{pmatrix} \right|^2 \\ &= \frac{\mathcal{V}^2}{8} \left| g_e B_\mu + g' \sigma^i W_\mu^i \begin{pmatrix} 0 \\ 1 \end{pmatrix} \right|^2 \\ &= \frac{\mathcal{V}^2}{8} \left| \begin{pmatrix} g' W_\mu^1 - i g' W_\mu^2 \\ g_e B_\mu - g' W_\mu^3 \end{pmatrix} \right|^2 \\ &= \frac{\mathcal{V}^2}{8} \left[ g'^2 \left( (W_\mu^1)^2 + (W_\mu^2)^2 \right) + (g' W_\mu^3 - g_e B_\mu)^2 \right] \end{aligned} \quad (2.28)$$

$$\begin{aligned} W_\mu^\pm &= \frac{1}{\sqrt{2}} (W_\mu^1 \mp i W_\mu^2) & \text{with mass} & \quad m_W = \frac{1}{2} g' \mathcal{V} \\ Z_\mu^0 &= \frac{1}{\sqrt{g_e^2 + g'^2}} (g' W_\mu^3 - g_e B_\mu) & \text{with mass} & \quad m_Z = \frac{1}{2} (\sqrt{g_e^2 + g'^2}) \mathcal{V} \end{aligned} \quad (2.29)$$

Weinberg angle  $\theta_W$  is used as

$$\cos\theta_W = \frac{g'}{\sqrt{g_e^2 + g'^2}} \quad \sin\theta_W = \frac{g_e}{\sqrt{g_e^2 + g'^2}} \quad (2.30)$$

The vector field which is orthogonal to  $Z_\mu^0$  will remain massless

$$A_\mu = \frac{1}{\sqrt{g_e^2 + g'^2}}(g_e W_\mu^3 + g' B_\mu) \quad \text{with mass} \quad m_A = 0 \quad (2.31)$$

At the end, after spontaneous symmetry break we have a real scalar Higgs field with three massively weak bosons,  $W^\pm$  and  $Z$  and one massless photon. The massless gauge field  $A_\mu$  is associated with the photon. It is the result of the fact that  $SU(2)_L \times U(1)_Y$  is broken into  $U(1)_Q$  symmetry.

### 2.2.5 Fermion masses, $\mathcal{L}_{Yukawa}$

We have built a term in  $\mathcal{L}$  which couples the Higgs doublet to fermion field. The yukawa section of the  $\mathcal{L}$  is given as

$$\begin{aligned} \mathcal{L}_{Yuk} &= Y_f [\bar{\psi}_L \phi \psi_R + \bar{\psi}_R \tilde{\phi} \psi_L] \\ \mathcal{L}_{Yuk} &= - \left( \bar{q}_L \cdot \tilde{\phi} \right) Y_u u_R - \left( \bar{q}_L \cdot \tilde{\phi} \right) Y_d d_R - \left( \bar{l}_L \cdot \phi \right) Y_L e_R + h.c., \end{aligned} \quad (2.32)$$

$e_R$ ,  $u_R$  and  $d_R$  are right handed leptons, right handed up and down type quarks respectively.

$$e_R = p_R e \quad , \quad u_R = p_R u \quad , \quad d_R = p_R d$$

$q_L$  and  $L_L^i$  are left handed quarks and left handed leptons respectively, where  $i = 1, 2, 3$  is the colour indices.

$$L_L = p_L \begin{pmatrix} \nu_{eL} \\ e_L \end{pmatrix} \quad , \quad q_L = p_L \begin{pmatrix} u_L \\ d_L \end{pmatrix}$$

where as

$$p_R = \frac{(1+\gamma_5)}{2} \quad \text{and} \quad p_L = \frac{(1-\gamma_5)}{2},$$

$Y_L$ ,  $Y_u$  and  $Y_d$  are  $3 \times 3$  general complex matrices that is yukawa coupling for lepton, up type and down type quarks respectively, leaving the  $h$  which is termed as Higgs boson mixed around the vacuum expectation value (VEV) as in Eq.(2.30), the Yukawa Lagrangian will look like,

$$\mathcal{L}_{Yuk} = -\frac{\mathcal{V}}{\sqrt{2}}\bar{u}_L Y_u u_R - \frac{\mathcal{V}}{\sqrt{2}}\bar{d}_L Y_d d_R - \frac{\mathcal{V}}{\sqrt{2}}\bar{e}_L Y_e e_R + \text{interactions} + h.c. \quad (2.33)$$

The fermions will gain finite mass if  $\phi$  has non zero VEV see Eq.(2.30). In general the Yukawa Lagrangian for three generations of leptons ( $\mathcal{L}_{Yuk}^{Lep}$ ) can be expressed as

$$\mathcal{L}_{Lep}^{Yuk} = \left( \bar{e}_R \quad \bar{\mu}_R \quad \bar{\tau} \right) Y_l \phi \begin{pmatrix} \begin{pmatrix} \nu_e \\ e \end{pmatrix}_L \\ \begin{pmatrix} \nu_\mu \\ \mu \end{pmatrix}_L \\ \begin{pmatrix} \nu_\tau \\ \tau \end{pmatrix}_L \end{pmatrix} + h.c \quad (2.34)$$

See the Eq.(2.37) the Yukawa coupling for fermions  $Y_l$  and fermion to Higgs field coupling can expressed as

$$Y_l = \sqrt{2}\left(\frac{m_l}{\mathcal{V}}\right) \quad , \quad \frac{Y_l}{\sqrt{2}} = \frac{m_l}{\mathcal{V}}$$

The Yukawa Lagrangian for the up and down types quarks are different as down type quarks ( $d, s, b$ ) get the mass by the Yukawa Lagrangian for down type quarks  $\mathcal{L}_{Yuk}^{d-Quarks} = Y_d \bar{\psi}_R \phi \psi_L$  that will be same as in Eq.(2.35) except the Yukawa coupling  $Y_d$ . Now the mass term for up type quarks ( $u, c, t$ ) take the form as

$$\mathcal{L}_{Yuk}^{u-Quarks} = Y_u \bar{\psi}_R \tilde{\phi} \psi_L + h.c$$

Where

$$\tilde{\phi} = -i\sigma_2 \phi^* = -\frac{1}{\sqrt{2}} \begin{pmatrix} \mathcal{V} + h \\ 0 \end{pmatrix}$$

$$\mathcal{L}_{Yuk}^{u-Quarks} = \left( \bar{u}_R \quad \bar{c}_R \quad \bar{t} \right) Y_u (i\sigma_2 \phi^*) \begin{pmatrix} \begin{pmatrix} u \\ d \end{pmatrix}_L \\ \begin{pmatrix} c \\ s \end{pmatrix}_L \\ \begin{pmatrix} t \\ b \end{pmatrix}_L \end{pmatrix} + h.c \quad (2.35)$$



$i\sigma_2\phi^*$  is  $SU(2)$  complex doublet where  $\sigma_2$  is pauli matrix. The mixed terms are still present, so in order to evaluate mass eigenstates, the states with proper mass terms, we diagonalize the Yukawa matrices  $Y^d$  and  $Y^u$  by mean of unitary matrices  $V^d$  and  $V^u$  respectively as fallow

$$Y_{diag}^q = V_L^q Y^q V_R^{q\dagger} \quad , \quad q = u, d$$

It is require that matrices  $V$  are unitary i-e  $V_L^q V_L^{q\dagger} = \mathbb{I}$ , then we redefine the field to eliminate the unitary matrices,

$$\begin{aligned} d_{Li} &= V_L^d d'_L, & d_{Ri} &= V_R^d d'_R \\ u_{Li} &= V_L^u u'_L, & u_{Ri} &= V_R^u u'_R \end{aligned} \quad (2.36)$$

These transformations convert the quark fields to the basis of mass eigenstates. This will allow to express quark interaction eigenstates  $d'$ ,  $u'$  as quark mass eigen state  $d$ ,  $u$ .

Now from Eq.(2.18) the charged current interaction among the left handed isospin doublet interaction eigenstates that are connected by  $W$  Boson can be written as,

$$\begin{aligned} \mathcal{L}_{cc}^{qL} &= \frac{g}{\sqrt{2}} \bar{u}_L \gamma_\mu W^{-\mu} d_L + \frac{g}{\sqrt{2}} \bar{d}_L \gamma_\mu W^{+\mu} u_L \\ \mathcal{L}_{cc}^{qL} &= \frac{g}{\sqrt{2}} \bar{u}'_L (V_L^u V_L^{d\dagger}) \gamma_\mu W^{-\mu} d'_L + \frac{g}{\sqrt{2}} \bar{d}'_L (V_L^d V_L^{u\dagger}) \gamma_\mu W^{+\mu} u'_L \end{aligned} \quad (2.37)$$

The combination of  $V_L^u V_L^{d\dagger}$  is a  $3 \times 3$  famous mixing matrix the Cabibbo Kobayashi Maskawa (CKM) matrix generally termed as  $V_{CKM}$  and will be discussed in chapter 3.

# Chapter 3

## Theoretical Formalism For Flavor And B Mesons Physics

In this chapter we will discuss the fermion sector of the SM, more precisely the quark sector and examine some of its important characteristics. To discuss the basic formalism of weak decays, we introduce the concept of Effective field theory (EFT).

### 3.1 Cabibbo Kobayashi Maskawa (CKM) matrix

In previous chapter we discussed the quark mass eigenstates, cf Eq.(2.40) which direct to the emergence of the CKM matrix.

$$V_{uL}V_{dL}^\dagger = V_{CKM} \tag{3.1}$$

The interaction eigen basis and the mass eigen basis are selected to be equal for the up-type quarks by convention, whereas the down-type quarks are selected to be rotated, going from the interaction basis to the mass basis,

$$\begin{aligned} Q'_d &= V_{CKM} Q_d \\ \begin{pmatrix} d' \\ s' \\ b' \end{pmatrix} &= \begin{pmatrix} V_{ud} & V_{us} & V_{ub} \\ V_{cd} & V_{cs} & V_{cb} \\ V_{td} & V_{ts} & V_{tb} \end{pmatrix} \begin{pmatrix} d \\ s \\ b \end{pmatrix} \end{aligned} \tag{3.2}$$

Therefore the members of  $V_{CKM}$  is written as follow [36]

$$V_{CKM} = \begin{pmatrix} V_{ud} & V_{us} & V_{ub} \\ V_{cd} & V_{cs} & V_{cb} \\ V_{td} & V_{ts} & V_{tb} \end{pmatrix} \quad (3.3)$$

In defining  $V_{CKM}$  we have more freedom by mean of which we can transform between the different generations. But this freedom is certain by arranging the up and down type quarks by means of their masses like

$$(u_1, u_2, u_3) \rightarrow (u, c, t) \quad ; \quad (d_1, d_2, d_3) \rightarrow (d, s, b) \quad (3.4)$$

Each member of the CKM matrix is evaluated experimentally [40] as

$$\begin{pmatrix} V_{ud} \approx 0.974 & V_{us} \approx 0.220 & V_{ub} \approx 0.003 \\ V_{cd} \approx 0.224 & V_{cs} \approx 0.969 & V_{cb} \approx 0.04 \\ V_{td} \approx 0.009 & V_{ts} \approx 0.042 & V_{tb} \approx 0.999 \end{pmatrix} \quad (3.5)$$

### 3.1.1 Standard Parametrization

The CKM matrix in terms of four parameters is parameterized in many way. The most popular representations the standard parametrization is given as

$$V_{CKM} = \begin{pmatrix} c_{12}c_{13} & s_{12}s_{13} & s_{13}e^{-i\delta} \\ -s_{12}c_{23} - c_{12}s_{23}s_{13}e^{i\delta} & c_{12}s_{23} - s_{12}s_{23}s_{13}e^{i\delta} & s_{23}c_{13} \\ s_{12}c_{23} - c_{12}s_{23}s_{13}e^{i\delta} & -s_{23}c_{12} - s_{12}c_{23}s_{13}e^{i\delta} & c_{23}c_{13} \end{pmatrix} \quad (3.6)$$

Here  $c_{ij} = \cos\theta_{ij}$  and  $s_{ij} = \sin\theta_{ij}$  while  $\delta$  is the phase, which varies in the range from  $0 \leq \delta \leq 2\pi$ . The four independent parameters are taken as

$$s_{12} = |V_{us}|, \quad s_{13} = |V_{ub}|, \quad s_{23} = |V_{cb}| \quad \text{and} \quad \delta.$$

The first three out of four can be taken out from the tree level decays moderated by the transitions  $s \rightarrow u$ ,  $b \rightarrow u$  and  $b \rightarrow c$  respectively. The phase  $\delta$  can be taken out from the charge parity (CP) violation transitions or loop processes which is sensitive to  $|V_{td}|$ . For numerical calculations the standard parametrization is exactly suitable.

### 3.1.2 Wolfenstein Parametrization

The one more parametrization that results more clearly is Wolfenstein parametrization, where expansion of elements is in small parameter  $\lambda = |V_{us}| \approx 0.22$  to  $\mathcal{O}(\lambda^3)$ , the matrix is given as

$$V_{CKM} = \begin{pmatrix} 1 - \frac{\lambda^2}{2} & \lambda & A\lambda^3(\rho - i\eta) \\ -\lambda & 1 - \frac{\lambda^2}{2} & A\lambda^2 \\ A\lambda^3(1 - \rho - i\eta) & -A\lambda^2 & 1 \end{pmatrix} + \mathcal{O}(\lambda^4) \quad (3.7)$$

Where the  $\lambda, A, \rho$  and  $\eta$  are the four new independent mixing parameters and in order to establish the relation to the parameter of the standard parametrization we taken it as

$$s_{12} \simeq \lambda \quad , \quad s_{23} \simeq A\lambda^2 \quad , \quad s_{13}e^{i\delta} \simeq A\lambda^3(\rho - i\eta). \quad (3.8)$$

Wolfenstein parametrization is a good estimation to the actual numerical values and some time used to express the hierarchical structure of the CKM matrix. The CKM matrix is more likely the unit matrix along off diagonal members that are small. The power of the  $\lambda$  will tell us the order of the magnitude for each term in Wolfenstein parametrization.

$$V_{CKM} \sim \begin{pmatrix} 1 & \lambda & \lambda^3 \\ \lambda & 1 & \lambda^2 \\ \lambda^3 & \lambda^2 & 1 \end{pmatrix} + \mathcal{O}(\lambda^4) \quad (3.9)$$

We perceive that the diagonal elements corresponds to quark transition inside a generation, are close to one, whereas the off diagonal elements corresponds to transitions among the generation, are small.

## 3.2 Weak Decays of Hadrons

The weak decays of hadrons occurs via weak interactions among quarks and these occurs at energies much lower than the scale of weak interactions  $\mathcal{O}(M_{W,Z})$ . Hence this phenomenon can be explained via low energy effective field theory.

The formation of the weak interaction in light of SM is quite simple. From Eq.(2.41) we can say the charged current coupling  $J_{CC}^\mu$  to  $W$  boson field mediates the flavour

changing decays. The  $J_{CC}^\mu$  having the left handed lepton and quark fields which is given as

$$J_{CC}^\mu = (\bar{u}_L, \bar{c}_L, \bar{t}_L) \gamma^\mu V_{CKM} \begin{pmatrix} d_L \\ s_L \\ b_L \end{pmatrix} + (\bar{\nu}_e, \bar{\nu}_\mu, \bar{\nu}_\tau) \begin{pmatrix} e_L \\ \mu_L \\ \tau_L \end{pmatrix} \quad (3.10)$$

In accordance with the form of the charged current interaction the weak decays of the meson may be classified into three types, the leptonic decay in which decaying meson quarks annihilate one another and in result only the leptons appear in the final state; non-leptonic decays, in which the final state contains only hadrons; and semi leptonic decays, in which both hadrons and leptons appear in the final state. We will focus on the semi leptonic decay in detail onwards regarding this thesis.

### 3.2.1 Effective Field Theory

In Quantum Field Theory (QFT) the Effective Field Theory (EFT) is used as a tool to deal with the multi-scale problems [38, 39, 41]. Consider a quantum field theory with a characteristic energy scale  $E$ , and suppose we are interested in the physics at some much lower scale  $T$  i.e. ( $T \ll E$ ). To construct an EFT we choose a cutoff  $\Lambda$  slightly below  $E$  and integrate out the heavy degrees of freedom from the theory, i.e., remove the particles which are heavier with respect to the cutoff scale  $\Lambda$ . The EFT contains only the relevant light degrees of freedom and thus can be regarded as a low energy limit of the full theory. The effective Lagrangian takes the form

$$\mathcal{L}_{eff} = \sum_{n \geq 0} C_n \mathcal{O}_n \quad (3.11)$$

It is an infinite sum over all local operators  $\mathcal{O}_n$  which are allowed by the symmetries of the theory, multiplied by coupling constants  $C_n$ , the so-called Wilson coefficients.

One may wonder how such a theory can be predictive. To answer this question we replace the coupling constants with dimensionless constants  $c_{i_n}$ . With this we can rewrite the Lagrangian,

$$\mathcal{L}_{eff} = \mathcal{L}_{(0)} + \sum_{n > 0} \sum_{i_n} \frac{c_{i_n}}{E^n} \mathcal{O}_{i_n} \quad (3.12)$$

The advantage of the new formula is easily seen. The higher the dimension of the operator, the more powers of  $E$  it is suppressed by. In other words, the lowest dimensional operators will be the most important ones. Depending on the precision goal one can truncate the series and thus only a finite number of operators and couplings need to be retained.

### 3.2.2 Operator Product Expansion

The Operator Product Expansion (OPE) is prescribe structure in order to define the weak interactions. Apply and study this process on a simple example  $c \rightarrow s u \bar{d}$  [43] the weak decay look figure below. The amplitude of the respective decay can be written

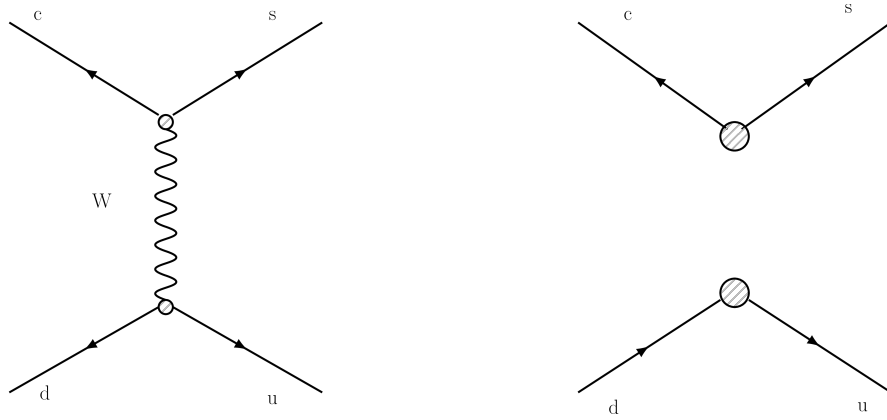


Figure 3.1:  $c \rightarrow s u \bar{d}$  in full and effective theory

as [45]

$$A_{full} = \frac{g'^2}{8} V_{ud} V_{cs}^* [\bar{u}_s(p_s) \gamma^\mu (1 - \gamma^5) u_c(p_c)] \frac{g_{\mu\nu}}{k^2 - M_W^2} [\bar{u}_u(p_u) \gamma^\nu (1 - \gamma^5) u_d(p_d)] \quad (3.13)$$

By introducing the Fermi constant  $G_F$  which is given as

$$\frac{G_F}{\sqrt{2}} = \frac{g'^2}{8M_W^2} \quad (3.14)$$

The Eq.(3.13) may look like as

$$A_{full} = \frac{G_F}{\sqrt{2}} V_{ud} V_{cs}^* [\bar{u}_s(p_s) \gamma^\mu (1 - \gamma^5) u_c(p_c)] \frac{M_W^2}{k^2 - M_W^2} [\bar{u}_u(p_u) \gamma_\mu (1 - \gamma^5) u_d(p_d)] \quad (3.15)$$

The amplitude may expand upto  $\mathcal{O}(k^2/M_W^2)$  like

$$A_{full} = \frac{G_F}{\sqrt{2}} V_{ud} V_{cs}^* [\bar{u}_s(p_s) \gamma^\mu (1 - \gamma^5) u_c(p_c)] [\bar{u}_u(p_u) \gamma^\nu (1 - \gamma^5) u_d(p_d)] + \mathcal{O}\left(\frac{k^2}{M_W^2}\right) \quad (3.16)$$

Since  $k$ , the momentum transfer through the  $W$  propagator, is small compared to  $M_W$ , terms of the order  $\mathcal{O}\left(\frac{k^2}{M_W^2}\right)$  can be safely neglected and the full amplitude can be approximated by the first term of the r.h.s of Eq.(3.15). The same result can be obtained from the effective Hamiltonian.

$$\mathcal{H}_{eff} = \frac{G_f}{\sqrt{2}} V_{ud} V_{cs}^* [\bar{s} \gamma^\mu (1 - \gamma^5) c] [\bar{u} \gamma_\mu (1 - \gamma^5) d] + \text{high dimension operators} \quad (3.17)$$

which agree with a low energy theory, in which the heavy particles have been integrated out. The higher dimensional operators correspond to the terms of order  $\mathcal{O}(k^2/M_W^2)$ .

This example shows the idea of the OPE, the non-local product of two charged current operators can be expanded into a series of local operators, whose contributions are weighted by effective coupling constants, the Wilson coefficients. Move on our example that is

$$A_{full} \stackrel{!}{=} A_{eff} = \frac{G_F}{\sqrt{2}} V_{cs}^* V_{ud} C \langle \mathcal{O} \rangle \quad (3.18)$$

By comparison the Wilson coefficient is equal to 1 and operator are given as

$$O = [\bar{s} \gamma^\mu (1 - \gamma^5) c] [\bar{u} \gamma_\mu (1 - \gamma^5) d] \quad (3.19)$$

### 3.2.3 Effective Hamiltonian

The dicussion for the weak hadron decay take starts from the effective Hamiltonian, whose general form can be written as

$$\mathcal{H}_{eff} = \frac{G_F}{\sqrt{2}} \sum_i V_{CKM}^i C_i(\mu) \mathcal{O}_i(\mu) \quad (3.20)$$

$G_F$  is the Fermi coupling constant.  $\mathcal{O}_i$  is a complete set of local operators relevant for the process. The CKM matrix elements and the Wilson coefficients describe the strength with which the operators enter the Hamiltonian. We observe that

both the Wilson coefficients and the local operators depend on the cutoff scale  $\mu$  (from now on  $\mu$  takes the role of the cutoff scale  $\Lambda$ ). All physics above this scale (high-energy effects) is absorbed into the Wilson coefficients, whereas low energy effects are contained in the local operators. In other words, the problem is separated in high and low energy regimes. This is the most important property of the OPE.

In order to compute the Wilson coefficients we have to choose an operator basis, i.e a set of operators, so that the effective Hamiltonian of each process can be expressed as a linear combination of these operators. Then the coefficients can be obtained by the requirement that the amplitude  $\mathcal{A}_{full}$  of the full theory is equal to the amplitude of the effective theory

$$A_{full} \stackrel{!}{=} A_{eff} = \frac{G_F}{\sqrt{2}} \sum_i V_{CKM}^i C_i(\mu) \langle \mathcal{O}_i(\mu) \rangle \quad (3.21)$$

The brackets presenting the matrix elements of the respective operators  $\mathcal{O}_i(\mu)$ . This procedure can be named as the matching of full theory with the effective theory. The full theory deals with all particles that appear in the process as dynamical degrees of freedom, whereas the effective theory is constructed by integrating out the heavy degrees of freedom (with respect to the cutoff scale). If the scale  $\mu$  is large enough, the matching can be done in perturbation theory. The Wilson coefficients will, in general, depend on the masses of the particles, which were integrated out.

The contribution of local operators and specially the effective operators in the Standard Model are summed up as follows [13].

### Current-Current Operators

$$\begin{aligned} \mathcal{O}_1 &= (\bar{s}_i \gamma^\mu (1 - \gamma^5) c_i) (\bar{c}_j \gamma^\mu (1 - \gamma^5) b_j) \\ \mathcal{O}_2 &= (\bar{s} \gamma^\mu (1 - \gamma^5) c) (\bar{c} \gamma^\mu (1 - \gamma^5) b) \end{aligned} \quad (3.22)$$



### QCD Penguin Operators

$$\begin{aligned}
\mathcal{O}_3 &= (\bar{s}\gamma^\mu(1 - \gamma^5)b)\Sigma_q(\bar{q}\gamma^\mu(1 - \gamma^5)q) \\
\mathcal{O}_4 &= (\bar{s}_i\gamma^\mu(1 - \gamma^5)b_j)\Sigma_q(\bar{q}_j\gamma^\mu(1 - \gamma^5)q_i) \\
\mathcal{O}_5 &= (\bar{s}\gamma^\mu(1 - \gamma^5)b)\Sigma_q(\bar{q}\gamma^\mu(1 + \gamma^5)q) \\
\mathcal{O}_6 &= (\bar{s}_i\gamma^\mu(1 - \gamma^5)b_j)\Sigma_q(\bar{q}_j\gamma^\mu(1 + \gamma^5)q_i)
\end{aligned} \tag{3.23}$$

### Magnetic Penguin Operators

$$\begin{aligned}
\mathcal{O}_7 &= \frac{em_b}{8\pi^2}(\bar{s}\sigma_{\mu\nu}(1 + \gamma^5)b)F_{\mu\nu} \\
\mathcal{O}_8 &= -\frac{g_s m_b}{8\pi^2}\bar{s}_i\sigma^{\mu\nu}(1 + \gamma^5)T^a b_j G_{\mu\nu}^a
\end{aligned} \tag{3.24}$$

### Semileptonic electroweak Penguin Operators

$$\begin{aligned}
\mathcal{O}_9 &= \frac{e}{8\pi^2}(\bar{s}\gamma^\mu(1 - \gamma^5)b)(\bar{l}\gamma^\mu l) \\
\mathcal{O}_{10} &= \frac{e}{8\pi^2}(\bar{s}\gamma^\mu(1 - \gamma^5)b)(\bar{l}\gamma^\mu\gamma_5 l).
\end{aligned} \tag{3.25}$$

Here  $i$  and  $j$  is for colour indices and  $\Sigma_q$  sum over the quarks such that  $q = u, d, s, c, b$ . The  $\mathcal{O}_{1,2}$  are current-current operators that define the weak decays structure and first order corrections as well, for example the  $W$  boson will has been taken into the coefficients  $C_1$  and  $C_2$ . The nuclear beta decay ( $n \rightarrow pe\bar{\nu}$ ) is one of the example. The operators  $\mathcal{O}_{3-6,8}$  will deal the loops including systems such that  $\mathcal{O}_{3-6}$  are QCD penguin operators and  $\mathcal{O}_{7,8}$  are magnetic penguin operators. Where the operators  $\mathcal{O}_7$ ,  $\mathcal{O}_9$  and  $\mathcal{O}_{10}$  are most meaningful regarding rare decays, where  $\mathcal{O}_{9,10}$  are semileptonic electroweak penguin operators [53].

### 3.2.4 Weak Decays of B Mesons

B physics has a very great importance in the particle physics that related with study the properties of B hadrons which must contain the one bottom quark at least. They are taken out by a charged  $W^+$  current, however have quite fascinating theoretical relations with the decays that are induced by loops.

The radiative electroweak penguin  $b \rightarrow s\gamma$  and  $b \rightarrow s\nu\bar{\nu}$  decays are of the great interest, that are the transition at quark level which cannot be traced directly as the quarks quickly form the Hadrons. Experimentally the exclusive decays are traced while the inclusive decay will be the sum of all the contributions. Occasionally the decay  $b \rightarrow s\gamma$  was first noticed by its exclusive decay  $B \rightarrow K^*\gamma$  [50]. The rare charm hadron decays are also probed but presently the experimental sensitivity is not enough to get the very low rates predicted in the SM.

The experimentally favoured are Exclusive decays but come along with great theoretical uncertainties, for example  $B^0 \rightarrow K^{*0}l^+l^-$  is well known [48]. The decay rate of this decay is hard to consider accurately, however observables that are describing the angular distribution of decay products can be more accurately predicted.

### 3.2.5 Rare B mesons decay

This section will concentrate on the rare decays of the mesons having  $b$  quarks [49]. Within the flavor physics the rare decays is an active field such that the research field studying the transformation of quarks from one class or flavour to other. The most convincingly produced  $b$  quark mesons are  $B^0$  which is composed of anti  $b$  quark and  $d$  quark, the  $B^+$  meson composed of  $\bar{b}$  and  $u$  quarks and  $B_s^0$  meson composed of  $\bar{b}$  and  $s$  quarks. The masses of these mesons are in range from 5 to 6 GeV/ $c^2$  that is six times the mass of proton but quite below from the mass of  $W$  boson that is of 80 GeV/ $c^2$  [54].

The more complicated process at quark level likely  $b \rightarrow d$  and  $b \rightarrow s$  transition do not occur in standard model at tree level because the  $Z$  boson coupling with quarks of distinct flavour does not take place [52].

In above figure the rare decay process like the  $B_s^0 \rightarrow \mu^+\mu^-$  carry out via a loop occasionally referred to as penguins shape. The process like this is rare as the probability of the transition rapidly decrease with the number of the electroweak vertices, usually two vertices in decays at the tree level and three or four vertices at loop level decays

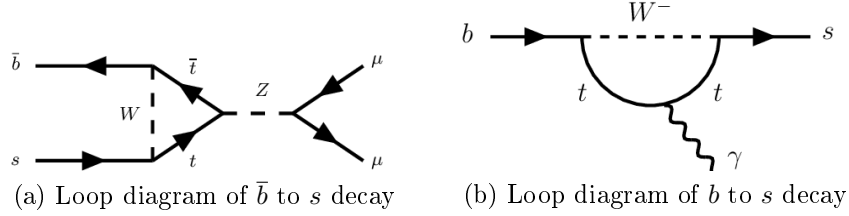


Figure 3.2: Change of flavour with the exchange of W boson.

along with the mediator particles which suppressed the decay more.

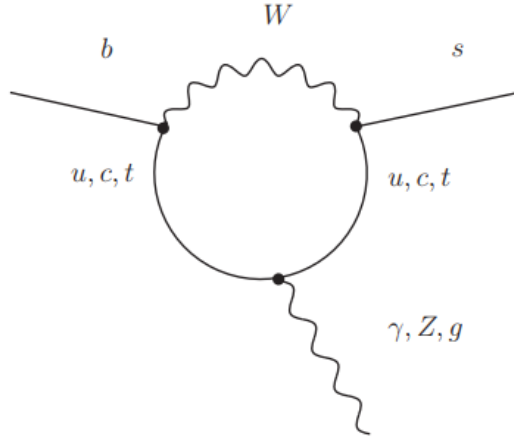
The Hadron's weak decays are moderated by weak interactions among the quarks, which take part at energies quite lower than the scale of weak interactions  $\mathcal{O}[M_{W,Z}]$ . So low energy effective theory will be used to deal with this.

### 3.3 Flavour Changing Neutral Currents

The flavour changing neutral current (FCNC) is forbidden at tree level in SM [46]. There is for example no direct coupling between the  $b$  quark and the  $s$  or  $d$  quarks. To understand why let us look at the  $Z$  boson current in the fermionic Lagrangian

$$J_Z^\mu \sim \bar{d}_L \gamma^\mu d_L \quad (3.26)$$

When we apply the field redefinitions, the unitary matrices just cancel out and thus there are no transitions between quarks of different generations. The same is true for the electromagnetic current. As we have already seen in Eq.(3.10), there are flavor changing charged currents in the SM. At loop level FCNCs can be induced through a W boson exchange.



(a) penguin diagram

Figure 3.3: Change of flavour with the exchange of W boson.

The FCNCs are important features of flavor physics. They not only allow measurements of the CKM matrix elements, but are also highly sensitive to New Physics. FCNCs are however strongly suppressed in the SM. This is ensured through the GIM mechanism.

### 3.3.1 GIM Mechanism

Glashow–Iliopoulos–Maiani (GIM) Mechanism was proposed by S.L. Glashow, J. Iliopoulos and L. Maiani in 1970. Its discovery involved the introduction of a fourth quark, the charm quark, which was still unknown at that time[10]. We can apply the GIM mechanism on the rare radiative B-meson decay which at quark level occurs as  $b \rightarrow s\gamma$ , cf.fig(3.3). The overall amplitude is the sum of the diagrams with  $u$ ,  $c$  and  $t$  in the loop.

$$\mathcal{A} = \mathcal{A}(m_u^2)V_{us}^*V_{ub} + \mathcal{A}(m_c^2)V_{cs}^*V_{cb} + \mathcal{A}(m_t^2)V_{ts}^*V_{tb} \quad (3.27)$$

We obtain from unitary CKM matrix that

$$V_{us}^*V_{ub} + V_{cs}^*V_{cb} + V_{ts}^*V_{tb} = 0 \quad (3.28)$$

Therefore If the quarks have the same masses in other words  $m_u = m_c = m_t$ , then amplitude would be zero and FCNCs would be prohibited though at loop level. But

we have the knowledge that the quarks vary in their masses and mainly  $m_t \gg m_u, m_c$ . The amplitude is in proportional to  $\ln(m_t^2/m_W^2)$  as the quark mass variation has break the cancellation. As long as top quark is so massive, then in result the loop diagrams are not suppressed so strongly and are anticipated to have considerable rates by mean of which Standard Model is testing.

### 3.4 Decay Amplitude for Hadronic Decays

An amplitudes for the decay of the initial state meson  $i$  into the final state meson is given in general as,

$$\mathcal{M}(i \rightarrow f) = \langle f | \mathcal{H}_{eff} | i \rangle = \frac{G_F}{\sqrt{2}} \sum_i V_{CKM}^i C_i(\mu) \langle f | \mathcal{O}_i(\mu) | i \rangle, \quad (3.29)$$

The  $\langle f | \mathcal{O}_i(\mu) | i \rangle$  are the hadronic matrix elements of  $\mathcal{O}_i$  among initial ( $i$ ) and final ( $f$ ) state. The scale  $\mu$  as discussed before differentiate the physics takes part into the short distance and long distance contributions deal with  $C_i(\mu)$  and  $\langle \mathcal{O}_i(\mu) \rangle$  respectively. Sometime these values base on unknown parameters of the theory like the masses of so far unseen new particles.

#### 3.4.1 Amplitude for Rare B decay at Quark Level

At quark level the decay of  $b \rightarrow sl^+l^-$  is a source of studies of New Physics on its own, here  $l = e, \mu$ . But these decays in the SM are included by the loop diagram like that of the  $b \rightarrow s\gamma$ . The loop diagram for  $b \rightarrow sl^+l^-$  is given as,

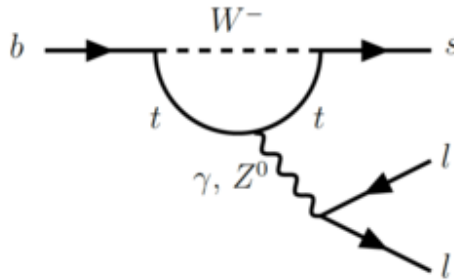


Figure 3.4: Electroweak Loop or penguin diagram for  $b \rightarrow sl^+l^-$  in SM dominant contributions.

The effective Hamiltonian guide to the  $b \rightarrow sl^+l^-$  quark decay amplitude is given as,

$$\begin{aligned} \mathcal{M}(b \rightarrow sl^+l^-) = & \frac{G_F \alpha}{2\sqrt{2}\pi} V_{ts}^* V_{tb} \left[ C_9^{eff} (\bar{s}\gamma^\mu(1 - \gamma^5)b)(\bar{l}\gamma^\mu l) \right. \\ & \left. + C_{10}(\bar{s}\gamma^\mu(1 - \gamma^5)b)(\bar{l}\gamma^\mu\gamma^5 l) - \frac{2m_b}{q^2} C_7^{eff} (\bar{s}i\sigma^{\mu\nu}q^\nu(1 + \gamma^5)b)(\bar{l}\gamma^\mu l) \right]. \end{aligned} \quad (3.30)$$

Usually the rare B decay are defines within the framework of an effective low energy theory that achieved by the integrate out the heavy degree of freedom, that are the  $W^\pm$  bosons and a top quark in this particular case. In respect of the SM, there are the effects of the  $W$ ,  $Z$  bosons and top( $t$ ) quark that are essentially removed from the theory and includes into the Willson coefficients. We will not take into account the operators except  $\mathcal{O}_{8g}$  because of not taking contribution of gluons here, where as operators up to six dimensions  $\mathcal{O}_i(i = 1, 2, \dots, 6)$  are taking into consideration and the effective operators  $\mathcal{O}_{7,9,10}$  contributes in the decays followed bt  $b \rightarrow sl^+l^-$  transitions.

# Chapter 4

## The Decay $B \rightarrow K_1(1270, 1400)\mu^+\mu^-$ in the Standard Model

In this chapter we analyze the physical observables such as branching ratios ( $\mathcal{BR}$ ), forward backward asymmetry ( $\mathcal{A}_{FB}$ ), helicity fractions ( $f_L$ ), unpolarized and polarized ratios ( $R_\mu$ ) via the Semi-leptonic rare B meson decay  $B \rightarrow K_1(1270, 1400)\mu^+\mu^-$  in the framework of SM.

### 4.1 Ingredients for $B \rightarrow K_1\mu^+\mu^-$

At quark level the decay  $B \rightarrow K_1\mu^+\mu^-$  is governed by  $b \rightarrow sl^+l^-$  transition. The effective Hamiltonian for such a decay can be expressed as

$$\mathcal{H}_{eff} = -\frac{4G_F}{\sqrt{2}}V_{ts}^*V_{tb} \left[ \sum_{i=1}^6 C_i(\mu)\mathcal{O}_i(\mu) + \sum_{i=7,9,10} C_i(\mu)\mathcal{O}_i(\mu) \right] \quad (4.1)$$

In the SM the  $\mathcal{H}_{eff}$  can be expressed like this after integrating out the heavy degrees of freedom in the full theory and left with the local quark operators  $\mathcal{O}_i$ , four quark and their correlating Wilson coefficients  $C_i(\mu)$  [69].

The amplitude for the said process can be obtained by sandwiching the effective Hamiltonian between initial and final state. Hence for the said decay the amplitudes

can read as follows,

$$\begin{aligned}
\mathcal{M}(B \rightarrow K_1 \mu^+ \mu^-) &= \frac{G_F \alpha}{2\sqrt{2}\pi} V_{ts}^* V_{tb} \left[ \langle K_1(k, \varepsilon) | \bar{s} \gamma^\mu (1 - \gamma^5) b | B(p) \rangle \{ C_9^{eff} (\bar{\mu} \gamma^\mu \mu) \right. \\
&\quad \left. + C_{10} (\bar{\mu} \gamma^\mu \gamma^5 \mu) \} - \frac{2m_b}{q^2} C_7^{eff} \langle K_1(k, \varepsilon) | \bar{s} i \sigma_{\mu\nu} q^\nu (1 + \gamma^5) b | B(p) \rangle (\bar{\mu} \gamma^\mu \mu) \right]
\end{aligned} \tag{4.2}$$

The  $K_1(1270, 1400)$  is final state axial vector meson. One can define the momenta as  $p = k + k_1 + k_2$  in which  $k_1$  and  $k_2$  are the momenta associate with the leptons  $\mu^+$  and  $\mu^-$  with  $p^2 = M_B^2$ ,  $k^2 = M_{K_1}^2$  and  $k_1^2 = k_2^2 = \mu$ , where  $m_1$ ,  $m_2$  and  $\mu$  are the masses associated with initial meson  $B$ , final state meson  $K_1$  and leptons that is muon here, respectively.

## 4.2 Form Factor And Mixing of $K_1(1270) - K_1(1400)$

The hadronic matrix elements of the quark operators for the exclusive decay  $B \rightarrow K_1(1270, 1400) \mu^+ \mu^-$  can be specified in terms of form factor is given as,

$$\begin{aligned}
\langle K_1(k, \varepsilon) | V_\mu | B(p) \rangle &= \varepsilon_\mu^* (M_B + M_{K_1}) V_1(q^2) - P_\mu(\varepsilon^* \cdot q) \frac{V_2(q^2)}{M_B + M_{K_1}} \\
&\quad - q_\mu(\varepsilon^* \cdot q) \frac{2M_{K_1}}{q^2} [V_3(q^2) - V_0(q^2)], \\
\langle K_1(k, \varepsilon) | A_\mu | B(p) \rangle &= -\frac{2i\epsilon_{\mu\nu\alpha\beta}}{M_B + M_{K_1}} \varepsilon^{*\nu} p^\alpha k^\beta A(q^2), \\
\langle K_1(k, \varepsilon) | \bar{s} i \sigma_{\mu\nu} q^\nu b | B(p) \rangle &= [(M_B^2 - M_{K_1}^2) \varepsilon_\mu^* - (\varepsilon^* \cdot q) P_\mu] F_2(q^2) \\
&\quad + (\varepsilon^* \cdot q) [q_\mu - \frac{q^2}{M_B^2 - M_{K_1}^2} P_\mu] F_3(q^2), \\
\langle K_1(k, \varepsilon) | \bar{s} i \sigma_{\mu\nu} q^\nu \gamma^5 b | B(p) \rangle &= 2i\epsilon_{\mu\nu\alpha\beta} \varepsilon^{*\nu} p^\alpha k^\beta F_1(q^2).
\end{aligned} \tag{4.3}$$

Here  $V^\mu = \bar{s} \gamma^\mu b$  is vector and  $A^\mu = \bar{s} \gamma^\mu \gamma^5 b$  is axial vector current,  $P_\mu = (p + k)_\mu$  and  $\varepsilon^{*\nu}$  are the polarization vector of axial vector meson. The relationship for vector



form factors in above equation are given as

$$\begin{aligned} V_3(q^2) &= \frac{M_B + M_{K_1}}{2M_{K_1}} V_1(q^2) - \frac{M_B - M_{K_1}}{2M_{K_1}} V_2(q^2) \\ V_3(0) &= V_0(0) \end{aligned} \quad (4.4)$$

Where  $q = p - k$ ,  $\gamma_5 = i\gamma^0\gamma^1\gamma^2\gamma^3$  and  $A$ ,  $V_i$  and  $F_i$  are the form factors whose values are specified in the table coming next. The  $K_1(1270)$  and  $K_1(1400)$  are the physical mixed states of  $K_{1A}$  and  $K_{1B}$  with mixing angle  $\theta_K$  can be define as

$$|K_1(1270)\rangle = |K_{1A}\rangle \sin \theta_{K_1} + |K_{1B}\rangle \cos \theta_{K_1} \quad (4.5)$$

$$|K_1(1400)\rangle = |K_{1A}\rangle \cos \theta_{K_1} - |K_{1B}\rangle \sin \theta_{K_1} \quad (4.6)$$

The mixing angle  $\theta_{K_1}$  has not been exactly established but it was approximated to be  $-(34 \pm 13)^\circ$  from the decay  $B \rightarrow K_1(1270)\gamma$  and  $\tau \rightarrow K_1(1270)\mu\tau$  [32]. Thus the different possibilities in this framework examine for  $\theta_{K_1}$ . The magnitude of  $\theta_{K_1}$  established here as  $34^\circ \leq \theta_{K_1} \leq 58^\circ$ . In respect of  $K_{1A}$  and  $K_{1B}$  the  $B \rightarrow K_1(1270, 1400)$  matrix elements can be specify in term of form factor as

$$\begin{pmatrix} \langle K_1(1270) | \bar{s}\gamma^\mu(1 - \gamma^5)b | B \rangle \\ \langle K_1(1400) | \bar{s}\gamma^\mu(1 - \gamma^5)b | B \rangle \end{pmatrix} = M \begin{pmatrix} \langle K_{1A} | \bar{s}\gamma^\mu(1 - \gamma^5)b | B \rangle \\ \langle K_{1B} | \bar{s}\gamma^\mu(1 - \gamma^5)b | B \rangle \end{pmatrix} \quad (4.7)$$

$$\begin{pmatrix} \langle K_1(1270) | \bar{s}\sigma_{\mu\nu}q^\nu(1 + \gamma^5)b | B \rangle \\ \langle K_1(1400) | \bar{s}\sigma_{\mu\nu}q^\nu(1 + \gamma^5)b | B \rangle \end{pmatrix} = M \begin{pmatrix} \langle K_{1A} | \bar{s}\sigma_{\mu\nu}q^\nu(1 + \gamma^5)b | B \rangle \\ \langle K_{1B} | \bar{s}\sigma_{\mu\nu}q^\nu(1 + \gamma^5)b | B \rangle \end{pmatrix} \quad (4.8)$$

Where  $M$  is the mixing or called as rotation matrix that can be written as

$$M = \begin{pmatrix} \sin \theta_K & \cos \theta_K \\ \cos \theta_K & -\sin \theta_K \end{pmatrix} \quad (4.9)$$

The form factors  $A^{K_1}$ ,  $V_{0,1,2}^{K_1}$  and  $F_{0,1,2}^{K_1}$  satisfies the following relation.

$$\begin{pmatrix} A^{K_1(1270)}/M_B + M_{K_1(1270)} \\ A^{K_1(1400)}/M_B + M_{K_1(1400)} \end{pmatrix} = M \begin{pmatrix} A^{K_{1A}}/M_B + M_{K_{1A}} \\ A^{K_{1B}}/M_B + M_{K_{1B}} \end{pmatrix} \quad (4.10)$$

$$\begin{pmatrix} (M_B + M_{K_1(1270)})V_1^{K_1(1270)} \\ (M_B + M_{K_1(1400)})V_1^{K_1(1400)} \end{pmatrix} = M \begin{pmatrix} (M_B + M_{K_{1A}})V_1^{K_{1A}} \\ (M_B + M_{K_{1B}})V_1^{K_{1B}} \end{pmatrix} \quad (4.11)$$

$$\begin{pmatrix} V_2^{K_1(1270)}/M_B + M_{K_1(1270)} \\ V_2^{K_1(1400)}/M_B + M_{K_1(1400)} \end{pmatrix} = M \begin{pmatrix} V_2^{K_1A}/M_B + M_{K_1A} \\ V_2^{K_1B}/M_B + M_{K_1B} \end{pmatrix} \quad (4.12)$$

$$\begin{pmatrix} M_{K_1(1270)}V_0^{K_1(1270)} \\ M_{K_1(1400)}V_0^{K_1(1400)} \end{pmatrix} = M \begin{pmatrix} M_{K_1A}V_0^{K_1A} \\ M_{K_1B}V_0^{K_1B} \end{pmatrix} \quad (4.13)$$

$$\begin{pmatrix} F_1^{K_1(1270)} \\ F_1^{K_1(1400)} \end{pmatrix} = M \begin{pmatrix} F_1^{K_1A} \\ F_1^{K_1B} \end{pmatrix} \quad (4.14)$$

$$\begin{pmatrix} (M_B^2 - M_{K_1(1270)}^2)F_2^{K_1(1270)} \\ (M_B^2 - M_{K_1(1400)}^2)F_2^{K_1(1400)} \end{pmatrix} = M \begin{pmatrix} (M_B^2 - M_{K_1A}^2)F_2^{K_1A} \\ (M_B^2 - M_{K_1B}^2)F_2^{K_1B} \end{pmatrix} \quad (4.15)$$

$$\begin{pmatrix} F_3^{K_1(1270)} \\ F_3^{K_1(1400)} \end{pmatrix} = M \begin{pmatrix} F_3^{K_1A} \\ F_3^{K_1B} \end{pmatrix} \quad (4.16)$$

**Table 4.1.** Form Factor [60] for  $B \rightarrow K_{1A,1B}$ , here  $x$  and  $y$  are the parameter of the form factor.

$\mathcal{H}_i^n(q^2)$	$\mathcal{H}(0)$	$x$	$y$	$\mathcal{H}_i^n(q^2)$	$\mathcal{H}(0)$	$x$	$y$
$V_0^{K_{1A}}$	0.22	2.40	1.78	$V_0^{K_{1B}}$	-0.45	1.34	0.690
$V_1^{K_{1A}}$	0.34	0.635	0.211	$V_1^{K_{1B}}$	-0.29	0.729	0.074
$V_2^{K_{1A}}$	0.41	1.51	1.18	$V_2^{K_{1B}}$	0.17	0.919	0.855
$A^{K_{1A}}$	0.45	1.60	0.974	$A^{K_{1B}}$	-0.37	1.72	0.912
$F_1^{K_{1A}}$	0.31	0.629	0.387	$F_1^{K_{1B}}$	-0.25	1.59	0.790
$F_2^{K_{1A}}$	0.31	0.629	0.387	$F_2^{K_{1B}}$	-0.25	0.378	-0.755
$F_3^{K_{1A}}$	0.28	1.36	0.720	$F_3^{K_{1B}}$	-0.11	1.61	10.2

The form factors that used for the study of the physical observable are evaluated in the framework of QCD light cone sum rules [60]. These results are applicable only at low  $q^2$  region. However to investigate the effects of observables on the whole kinematical region, the form factors can be parameterized in the three-parameter form as

$$\mathcal{H}_i^n(q^2) = \frac{\mathcal{H}_i^n(0)}{1 - x_i^n(q/m_B^2) + y_i^n(q^2/m_B^2)^2} \quad (4.17)$$

The  $\mathcal{H}$ ,  $A$ ,  $V$ , and  $F$  are form factors whose numerical values are mentioned in table 4.1, here  $i$  will have the value either 0, 1, 2, or 3 and  $n$  is use for  $K_{1A}$  or  $K_{1B}$  states.

The Wilson coefficients used in the calculations are [58, 70],

**Table 4.2.** Wilson Coefficients  $C_i^\mu$  in th Standard Model at the scale  $\mu \sim m_b$

$C_1$	$C_2$	$C_3$	$C_4$	$C_5$	$C_6$	$C_7$	$C_9$	$C_{10}$
-0.263	1.011	0.005	-0.0806	0.0004	0.0009	-0.2923	4.0749	-4.3085

The matrix elements in Eq.(4.11) can be simplified from [58] as,

$$\mathcal{M} = \frac{G_F \alpha}{2\sqrt{2}\pi} \lambda_t \{ I_1^\mu \bar{\mu} \gamma^\mu \mu + I_2^\mu \bar{\mu} \gamma^\mu \gamma^5 \mu \}, \quad (4.18)$$

$I_i^\mu$  is given as

$$I_j^\mu = I_j^{\mu\nu} \epsilon_\nu^* \quad \text{Where} \quad j = 1, 2 \quad (4.19)$$

The Wilson coefficients and form factors are expressed in the form of auxiliary funtions as

$$\begin{aligned} I_1^{\mu\nu} &= i\epsilon_{\mu\nu\alpha\beta} p^\alpha k^\beta \mathcal{I}_1(q^2) + g_{\mu\nu} \mathcal{I}_2(q^2) - q_\mu q_\nu \mathcal{I}_3(q^2) - P_\mu q_\nu \mathcal{I}_4(q^2) \\ I_2^{\mu\nu} &= i\epsilon_{\mu\nu\alpha\beta} p^\alpha k^\beta \mathcal{I}_5(q^2) + g_{\mu\nu} \mathcal{I}_6(q^2) - q_\mu q_\nu \mathcal{I}_7(q^2) - P_\mu q_\nu \mathcal{I}_8(q^2) \end{aligned} \quad (4.20)$$

Where  $\mathcal{I}_i$  ( $i = 1, \dots, 8$ ) are the auxiliary function that includes both the Wilson coefficients and form factors and expressed explicitly as

$$\begin{aligned} \mathcal{I}_1(q^2) &= 2C_9^{eff} \frac{A(q^2)}{M_B + M_{K_1}} + \frac{4m_b}{q^2} C_7^{eff} F_1(q^2) \\ \mathcal{I}_2(q^2) &= C_9^{eff} (M_B + M_{K_1}) V_1(q^2) + \frac{2m_b}{q^2} C_7^{eff} (M_b^2 - M_{K_1}^2) F_2(q^2) \\ \mathcal{I}_3(q^2) &= 2C_9^{eff} \frac{M_{K_1}}{q^2} (V_3(q^2) - V_0(q^2)) - \frac{2m_b}{q^2} C_7^{eff} F_3(q^2) \\ \mathcal{I}_4(q^2) &= C_9^{eff} \frac{V_2(q^2)}{M_B + M_{K_1}} - \frac{2m_b}{q^2} C_7^{eff} \left( F_2(q^2) - \frac{q^2}{M_B^2 - M_{K_1}^2} F_3(q^2) \right) \\ \mathcal{I}_5(q^2) &= 2C_{10}^{SM} \frac{A(q^2)}{M_B + M_{K_1}} \\ \mathcal{I}_6(q^2) &= c_{10}^{SM} (M_B + M_{K_1}) V_1(q^2) \\ \mathcal{I}_7(q^2) &= 2C_{10}^{SM} \frac{M_{K_1}}{q^2} (V_3(q^2) - V_0(q^2)) \\ \mathcal{I}_8(q^2) &= C_{10}^{SM} \frac{V_2(q^2)}{M_B + M_{K_1}} \end{aligned} \quad (4.21)$$

As mentioned earlier the final state  $K_1(1270)$  and  $K_1(1400)$  mesons contains mixing angle  $\theta_K$ .

The form factor can be expressed in terms of mixing angles as, for  $B \rightarrow K_1(1270)\mu^+\mu^-$  can be expressed as

$$\begin{aligned} A(q^2) &= -A^{K_{1A}} \sin \theta_K + A^{K_{1B}} \cos \theta_K, \\ F_i(q^2) &= -F_i^{K_{1A}} \sin \theta_K + F_i^{K_{1B}} \cos \theta_K, \\ V_i(q^2) &= -V_i^{K_{1A}} \sin \theta_K + V_i^{K_{1B}} \cos \theta_K. \end{aligned} \quad (4.22)$$

Form factors for  $B \rightarrow K_{1(1400)}$  in term of  $\theta_K$  is given as

$$\begin{aligned} A(q^2) &= A^{K_{1A}} \cos \theta_K - A^{K_{1B}} \sin \theta_K, \\ F_i(q^2) &= F_i^{K_{1A}} \cos \theta_K - F_i^{K_{1B}} \sin \theta_K, \\ V_i(q^2) &= V_i^{K_{1A}} \cos \theta_K - V_i^{K_{1B}} \sin \theta_K. \end{aligned} \quad (4.23)$$

The Wilson coefficients  $C_7^{eff}(\mu)$  and  $C_9^{eff}(\mu)$  take into consideration effectively which is given as in [14, 56]

$$C_9^{eff} = C_9 + X_{SD}(y, \hat{s}) + X_{LD}(y, \hat{s}), \quad (4.24)$$

where as  $y = m_c/m_b$ ,  $\hat{s} = q^2/m_b^2$ .  $X_{SD}(y, \hat{s})$  and  $X_{LD}(y, \hat{s})$  can expressed as

$$\begin{aligned} X_{SD}(y, \hat{s}) &= h(y, \hat{s})C_0 - \frac{1}{2}h(1, \hat{s})(4C_3 + 4C_4 + 3C_5 + C_6) - \frac{1}{2}h(0, \hat{s})(C_3 + 3C_4) \\ &\quad + \frac{2}{9}(3C_3 + C_4 + 3C_5 + C_6) \end{aligned} \quad (4.25)$$

The other terms are givenv as

$$\begin{aligned} h(y, \hat{s}) &= -\frac{8}{9} \ln \frac{m_b}{\mu} - \frac{8}{9} \ln y + \frac{8}{27} + \frac{4}{9}x \\ &\quad - \frac{2}{9}(2+x)|1-x|^{1/2} \begin{cases} (\ln |\frac{\sqrt{1-x}+1}{\sqrt{1-x}-1}| - i\pi), & \text{if } x \equiv \frac{4y}{\hat{s}} < 1, \\ 2\arctan \frac{1}{\sqrt{x-1}}, & \text{if } x \equiv \frac{4y}{\hat{s}} > 1, \end{cases} \\ h(0, s) &= \frac{8}{27} - \frac{8}{9} \ln \frac{m_b}{\mu} - \frac{4}{9} \ln \hat{s} - \frac{4}{9}i\pi. \end{aligned} \quad (4.26)$$

and

$$\begin{aligned} X_{LD}(y, \hat{s}) &= C_0 \frac{3\pi}{\alpha^2} \kappa \sum_{U_i=\psi_i} \frac{\Gamma(U_i \rightarrow l^+ l^-) m_{U_i}}{m_{U_i}^2 - q^2 - im_{U_i} \Gamma_{U_i}} \\ C_0 &\equiv 3C_1 + C_2 + 3C_3 + C_4 + 3C_5 + C_6 \end{aligned} \quad (4.27)$$

where  $\kappa = 1/C_0$  here.  $X_{SD}(y, \hat{s})$  and  $X_{LD}(y, \hat{s})$  represent the short and long distance contribution from four quark operators far away and near the  $c\bar{c}$  resonance regions respectively.  $X_{SD}$  can be evaluated certainly in the perturbative theory and  $X_{LD}$  may not be calculated from first QCD principles and by use of the quark hadron duality and vacuum saturation approximation, and can be parameterized in term of a phenomenological Breit-Wigner formula. Regardless of this, from the charm loop the nonfactorizable effects can bring about more corrections to decay  $b \rightarrow s\gamma$ , that can be absorbed into the effective Wilson coefficient  $C_7^{eff}(\mu)$  that can be expressed from [57].

$$C_7^{eff} = C_7 + C_{b \rightarrow s\gamma}$$

Where

$$C_{b \rightarrow s\gamma} = i\alpha_s \left[ \frac{2}{9} \eta^{14/23} (Q_1(x_t) - 0.1687) - 0.03C_2 \right] \quad (4.28)$$

$$Q_1(x) = \frac{x(x^2 - 5x - 2)}{8(x-1)^3} + \frac{3x^2 \ln^2 x}{4(x-1)^4},$$

here  $\eta = \alpha_s(m_W)/\alpha_s(\mu)$  and  $x = m_t^2/m_W^2$ .  $C_{b \rightarrow s\gamma}$  is the dropped part of rescattering  $b \rightarrow s c \bar{c} \rightarrow s\gamma$  and we have left out the little contributions propotional to the CKM part  $V_{ub}V_{us}^*$

### 4.3 Helicity Amplitudes

The Helicity Amplitudes in term of the auxiliary function is calculated from [32] can be expressed as [31],

$$H_1(\pm) = -\mathcal{I}_2 \pm \frac{1}{2} \mathcal{I}_1 \sqrt{(M_B^2 + M_{K_1}^2 - q^2)^2 - 4M_B^2 M_{K_1}^2}$$

$$H_2(\pm) = -\mathcal{I}_6 \pm \frac{1}{2} \mathcal{I}_5 \sqrt{(M_B^2 + M_{K_1}^2 - q^2)^2 - 4M_B^2 M_{K_1}^2}$$

$$H_1(0) = \frac{1}{2\sqrt{q^2} M_{K_1}} [\mathcal{I}_2(-M_B^2 + M_{K_1}^2 + q^2) + \mathcal{I}_4(M_B^4 - 2M_B^2(M_{K_1}^2 + q^2) + (M_{K_1}^2 - q^2)^2)]$$

$$H_2(0) = \frac{1}{2\sqrt{q^2} M_{K_1}} [\mathcal{I}_6(-M_B^2 + M_{K_1}^2 + q^2) + \mathcal{I}_8(M_B^4 - 2M_B^2(M_{K_1}^2 + q^2) + (M_{K_1}^2 - q^2)^2)] \quad (4.29)$$

## 4.4 Physical Observables

The branching ratio ( $\mathcal{BR}$ ),  $d\Gamma(B \rightarrow K_1 \mu^+ \mu^-)/dq^2$ , forward-backward Asymmetry  $A_{FB}$ , longitudinal helicity fractions  $f_L$ , unpolarized ratio ( $R_\mu(K_1)$ ), longitudinal and transverse ratios ( $R_\mu^{(L,T)}(K_1)$ ) are plotted in figures below, to check the dependence on the angle  $\theta_{K_1}$  for different angle  $\theta_{K_1} = -34^\circ, -45^\circ$  and  $-57^\circ$  respectively.

### 4.4.1 Differential Decay Rate ( $\frac{d\Gamma}{dq^2}$ )

The branching ratio  $\mathcal{BR}$  for the  $B \rightarrow K_1 \mu^+ \mu^-$  can be expressed as

$$\frac{d\Gamma(B \rightarrow K_1 \mu^+ \mu^-)}{dq^2} = \frac{G_F^2 \lambda_t^2 \alpha^2 \sqrt{\lambda}}{2^{11} \pi^5 M_B^3} \sqrt{1 - 4m_l^2/q^2} \times |\mathcal{M}|^2. \quad (4.30)$$

After simplification the amplitude can be expressed as,

$$|\mathcal{M}|^2 = \frac{8}{3}(q^2 + 2m_l^2)H^{(1)}H^{\dagger(1)} + \frac{8}{3}(q^2 - 4m_l^2)H^{(2)}H^{\dagger(2)}. \quad (4.31)$$

So the  $\mathcal{BR}$  for the  $B \rightarrow K_1 \mu^+ \mu^-$  in helicity basis can expressed as,

$$\begin{aligned} \frac{d\Gamma(B \rightarrow K_1 \mu^+ \mu^-)}{dq^2} = & \frac{G_F^2 \lambda_t^2 \alpha^2 q^2 \sqrt{\lambda}}{(2\pi)^5 24M_B^3} \sqrt{1 - 4m_l^2/q^2} [(1 + 2m_l^2/q^2)H^{(1)}H^{\dagger(1)} \\ & + (1 - 4m_l^2/q^2)H^{(2)}H^{\dagger(2)}] \end{aligned} \quad (4.32)$$

$$H^{(i)}H^{\dagger(i)} = H_+^{(i)}H_+^{\dagger(i)} + H_-^{(i)}H_-^{\dagger(i)} + H_0^{(i)}H_0^{\dagger(i)}$$

where  $\lambda$  is define as,

$$\lambda = M_B^4 + M_{K_1}^4 + q^4 - 2M_B^2 M_{K_1}^2 - 2M_{K_1}^2 q^2 - 2q^2 M_B^2 \quad (4.33)$$

The  $\mathcal{BR}$  for our said process has been plotted separately for  $K_1(1270)$  and  $K_1(1400)$  in the figures 4.1. The compulsive scenario is complex by dependence on  $q^2$ , the dilepton mass squared.

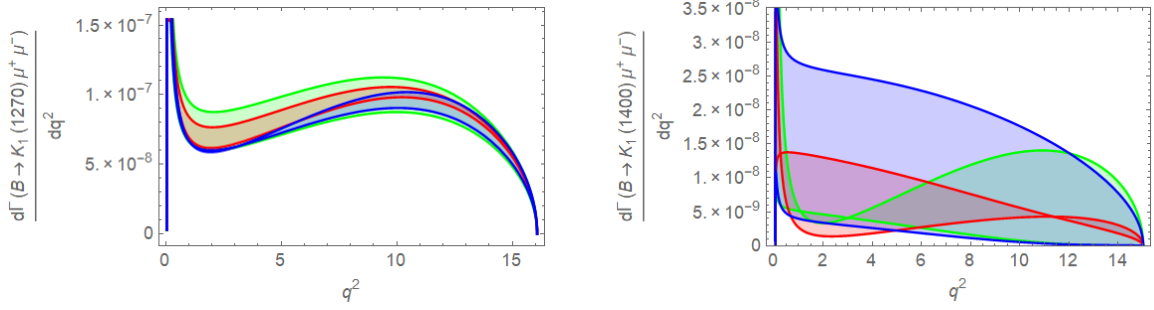


Figure 4.1: Branching ratio for the decay  $B \rightarrow K_{1(1270)}\mu^+\mu^-$  and  $B \rightarrow K_{1(1400)}\mu^+\mu^-$  in Standard Model. The green, red and blue curves belongs to angles  $\theta_{K_1} = -34^\circ, -45^\circ, -57^\circ$  with positive and negative uncertainties in the form factor.

Where we saw that at the low  $q^2$  region, that is  $q^2 \approx 2 \text{ GeV}^2$  the differential decay rate for  $B \rightarrow K_{1(1270)}\mu^+\mu^-$  decay are not so effective by the variation of  $\theta_{K_1}$ . Notice that in the low- $q^2$  region the distribution is dominated by the  $1/q^2$ , occasionally the  $\mathcal{BR}$  for the  $B \rightarrow K_{1(1270)}\mu^+\mu^-$  decay, put up contribution about 30% at around  $q^2 = 2 \text{ GeV}^2$  for  $-34^\circ \leq \theta_{K_1} \leq -57^\circ$ , where the  $\mathcal{BR}$  for the decay  $B \rightarrow K_{1(1400)}\mu^+\mu^-$  is enhanced by approximately 80% with  $\theta_{K_1} = -57^\circ$  as compared to  $\theta_{K_1} = -34^\circ$ . So we observed the deviation in the distribution for the process  $B \rightarrow K_{1(1400)}\mu^+\mu^-$  as compare to the  $B \rightarrow K_{1(1270)}\mu^+\mu^-$  at different angle  $\theta_{K_1}$ .

#### 4.4.2 Forward Backward Asymmetry

In the SM the zero position in the forward-Backward asymmetry ( $\mathcal{A}_{FB}$ ) exclusively based on the Wilson coefficients [58] that relate to the short distance physics. The differential  $\mathcal{A}_{FB}$  of the leptons is evaluated from the [66, ?]

$$\frac{d\mathcal{A}_{FB}(q^2)}{dq^2} = \int_0^1 \frac{d^2\Gamma}{dq^2 d\cos\theta} d\cos\theta - \int_{-1}^0 \frac{d^2\Gamma}{dq^2 d\cos\theta} d\cos\theta. \quad (4.34)$$

The  $\mathcal{A}_{FB}$  is evaluated as given below,

$$\mathcal{A}_{FB} = \frac{\int_0^1 \frac{d^2\Gamma}{dq^2 d\cos\theta} d\cos\theta - \int_{-1}^0 \frac{d^2\Gamma}{dq^2 d\cos\theta} d\cos\theta}{\int_{-1}^0 \frac{d^2\Gamma}{dq^2 d\cos\theta} d\cos\theta + \int_0^1 \frac{d^2\Gamma}{dq^2 d\cos\theta} d\cos\theta} \quad (4.35)$$

The differential form of the  $\mathcal{A}_{FB}$  is the given as,

$$\frac{d\mathcal{A}_{FB}(q^2)}{dq^2} = -\frac{G_F^2 \lambda_t^2 \alpha^2}{(2\pi)^5} \frac{q^2 \sqrt{\lambda}}{32M_B^3} (1 - 4m_l^2/q^2) \left[ H_+^{(1)} H_+^{(2)} + H_-^{(2)} H_-^{(1)} \right], \quad (4.36)$$

$H_1$  and  $H_2$  are defined in the eq.(4.33). The  $\mathcal{A}_{FB}$  explicitly expressed in term of Helicity Amplitudes as,

$$\mathcal{A}_{FB} = \frac{3}{4} \sqrt{1 - 4m_l^2/q^2} \left[ \frac{H_+^{(1)} H_+^{\dagger(2)} + H_-^{(2)} H_-^{\dagger(1)}}{(1 + 2m^2/q^2)H^{(1)}H^{\dagger(1)} + (1 - 4m^2/q^2)H^{(2)}H^{\dagger(2)}} \right]. \quad (4.37)$$

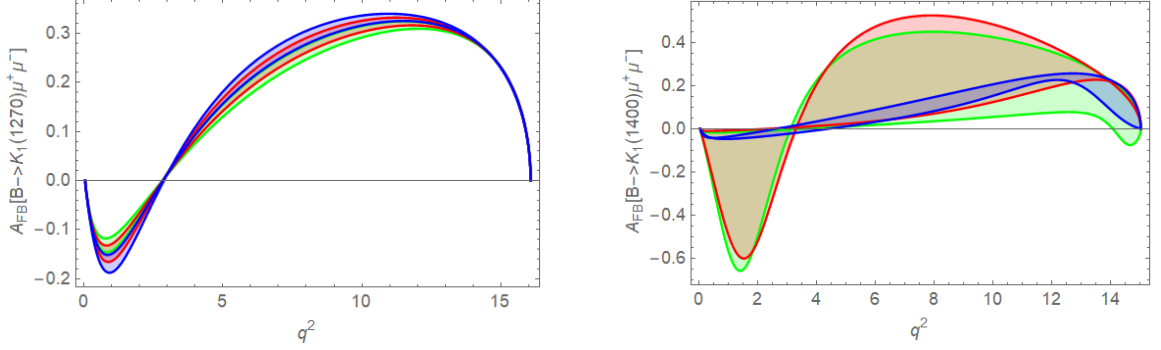


Figure 4.2: Forward-Backward Asymmetry for  $B \rightarrow K_1(1270)\mu^+\mu^-$  and  $B \rightarrow K_1(1400)\mu^+\mu^-$ . The green, red and blue curves belongs to angles  $\theta_{K_1} = -34^\circ, -45^\circ, -57^\circ$  with positive and negative uncertainties in the form factor.

We have plotted the  $\mathcal{A}_{FB}$  for our said process in SM. The  $B \rightarrow K_1(1270)\mu^+\mu^-$  decay is not sensitive to mixing angle as there is no shift in the zero value of the  $\mathcal{A}_{FB}$  in the plot at different mixing angle  $\theta_{K_1} = -34^\circ, -45^\circ, -57^\circ$  as we can observe that for each mixing angle the zero value of the  $\mathcal{A}_{FB}$  is at  $q^2 = 3\text{GeV}^2$  as shown in fig 4.2. Where as the  $B \rightarrow K_1(1400)\mu^+\mu^-$  decay shows the dependence on the mixing angle  $\theta_{K_1} = -34^\circ, -45^\circ, -57^\circ$ . Green curve is for  $\theta_{K_1} = 34^\circ$  whose zero value of  $\mathcal{A}_{FB}$  is at  $q^2 \leq 3\text{GeV}^2$ , where as red curve is for  $\theta_{K_1} = 45^\circ$  whose zero value of  $\mathcal{A}_{FB}$  is at  $3.5\text{GeV}^2 \leq q^2 \leq 4.5\text{GeV}^2$ , shifted toward right of zero value of  $\mathcal{A}_{FB}$  of green curve and for mixing angle  $\theta_{K_1} = 57^\circ$  the zero value of  $\mathcal{A}_{FB}$  of blue curve is at  $1.5\text{GeV}^2 \leq q^2 \leq 2.5\text{GeV}^2$  that shifted left to the green curve zero value of forward backward asymmetry. So the decay  $B \rightarrow K_1(1400)$  may be one the good mean in order to study effect.



### 4.4.3 Longitudinal Helicity Fraction

We now discuss helicity fractions of  $K_1(1270, 1400)$  meson in  $B \rightarrow K_1 \mu^+ \mu^-$  which are interesting observables and are insensitive to the uncertainties arising due to form factors and other input parameters. Thus the helicity fractions can be a good tool to test the physics within the framework of the SM. The longitudinal helicity fraction is given as the longitudinal partial decay rate divided by the total decay rate

$$f_L(q^2) = \frac{d\Gamma_L(q^2)/dq^2}{d\Gamma(q^2)/dq^2} \quad (4.38)$$

The final state meson helicity fractions were already discussed in the literature for  $B \rightarrow K^*(K_1) l^+ l^-$  decays [67]. The explicit expression of the longitudinal helicity fractions ( $f_L$ ) for  $B \rightarrow K_1 \mu^+ \mu^-$  decay can be obtained by trading  $|\mathcal{M}|$  to  $|\mathcal{M}_L|$  [68].

Thus we obtain the longitudinal differential decay rate as,

$$\frac{d\Gamma_L}{dq^2} = \frac{G_F^2 \lambda_t^2 \alpha^2}{(2\pi)^5} \frac{q^2 \sqrt{\lambda}}{24M_B^3} \sqrt{1 - 4m_l^2/q^2} [(1 + 2m_l^2/q^2) H_0^{(1)} H_0^{\dagger(1)} + (1 - 4m_l^2/q^2) H_0^{(2)} H_0^{\dagger(2)}], \quad (4.39)$$

By using the values in Eq.(4.38) we can evaluate the longitudinal helicity fraction as

$$f_L(q^2) = \frac{[(1 + 2m_l^2/q^2) H_0^{(1)} H_0^{\dagger(1)} + (1 - 4m_l^2/q^2) H_0^{(2)} H_0^{\dagger(2)}]}{[(1 + 2m_l^2/q^2) H^{(1)} H^{\dagger(1)} + (1 - 4m_l^2/q^2) H^{(2)} H^{\dagger(2)}]} \quad (4.40)$$

while the average value of  $f_L$  in the full  $q^2$  range for  $B \rightarrow K^* l^+ l^-$  is [61],

$$f_L = 0.63_{-0.19}^{+0.18} \pm 0.05 \quad q^2 \geq 0.1 \text{ GeV}^2$$

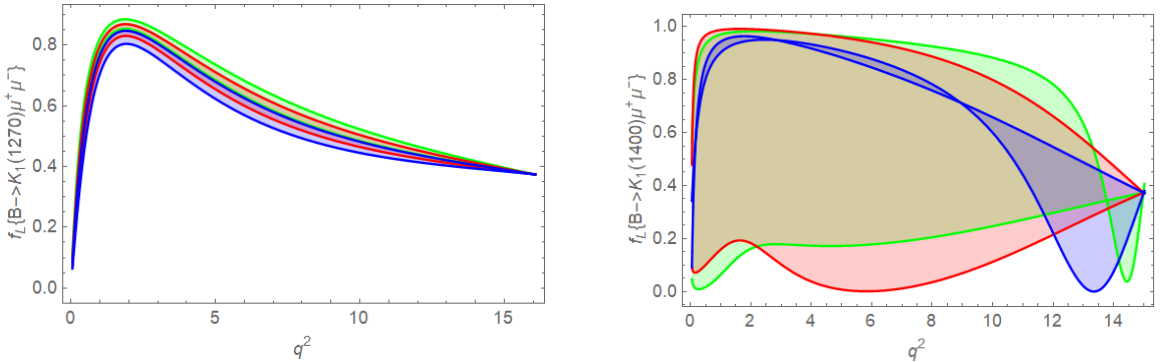


Figure 4.3: longitudinal Helicity Amplitude for the decay  $B \rightarrow K_1(1270) \mu^+ \mu^-$  and  $B \rightarrow K_1(1400) \mu^+ \mu^-$ . The green, red and blue curves belongs to angles  $\theta_{K_1} = -34^\circ, -45^\circ, -57^\circ$  with positive and negative uncertainties in the form factor.

Figs.(4.3) show the longitudinal helicity fraction ( $f_L$ ) of  $K_1(1270)$  and  $K_1(1400)$  for the decay  $B \rightarrow K_1(1270, 1400)\mu^+\mu^-$  as a function of  $q^2$  in SM, where we have used the light cone QCD sum rules form factors mentioned in table.(4.1). Just to see their dependence on the choice of the mixing angle  $\theta_{K_1}$  and form factors with positive and negative uncertainties we have plotted the  $f_L$ . Choosing the different values of the  $\theta_{K_1}$  i.e  $-34^\circ$ ,  $-45^\circ$  and  $-57^\circ$  we have observe from these figures that the effect are visible at low- $q^2$  region. In this case  $f_L$  interfere not very constructively for the case of  $K_1(1270)$  as compare to the  $K_1(1400)$ . Here one can see that the  $f_L$  of the final state meson  $K_1(1400)$  have dependence on the choice of form factors and  $\theta_{K_1}$  effects are quite significant in order to study the effects in SM as compare to  $K_1(1270)$ .

#### 4.4.4 $K_1(1400)$ to $K_1(1270)$ Ratio, ( $R_\mu(K_1)$ )

The ratio  $R_\mu(K_1) = \mathcal{B}(B \rightarrow K_1(1400)\mu^+\mu^-) / \mathcal{B}(B \rightarrow K_1(1270)\mu^+\mu^-)$ , longitudinal ratio  $R_\mu^L(K_1)$  and transverse ratio  $R_\mu^T(K_1)$ , as a function of  $\theta_{K_1}$  are given as

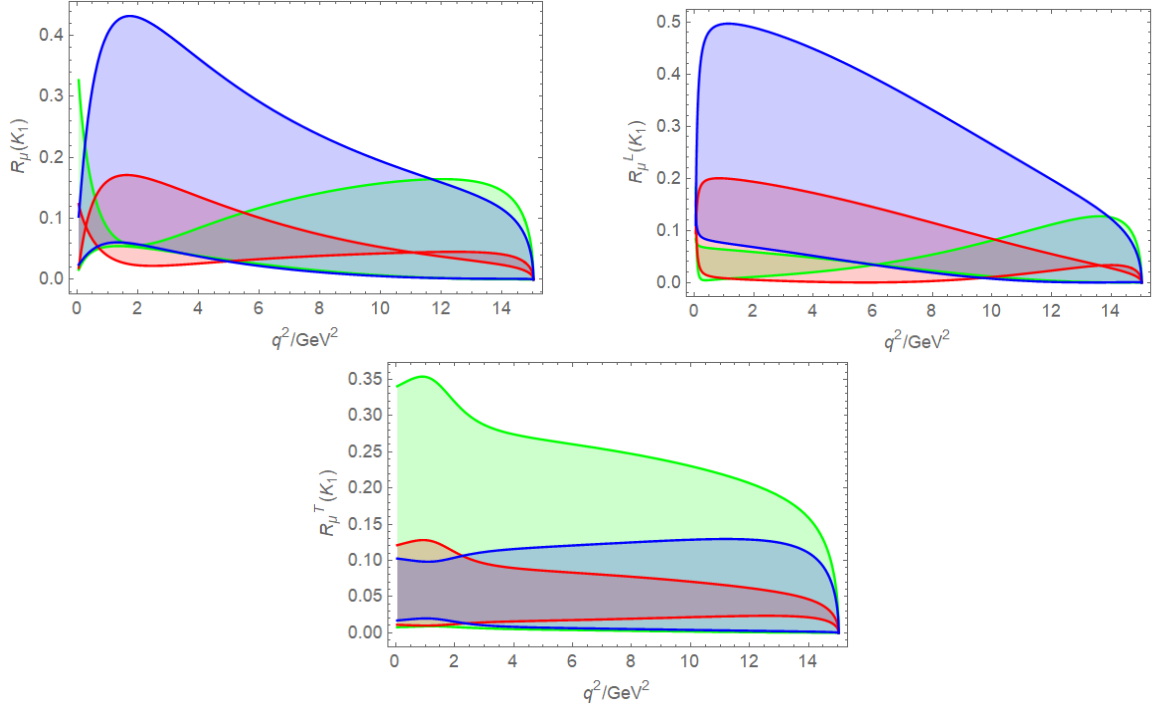


Figure 4.4: The  $R_\mu(K_1) = \mathcal{B}(B \rightarrow K_1(1400)\mu^+\mu^-) / \mathcal{B}(B \rightarrow K_1(1270)\mu^+\mu^-)$  with longitudinal  $R_\mu^L(K_1)$  and transverse  $R_\mu^T(K_1)$  ratio, as a function of  $\theta_{K_1}$ . The green, red and blue curves belongs to angles  $\theta_{K_1} = -34^\circ, -45^\circ, -57^\circ$  with positive and negative uncertainties in the form factor.

We observed the variation for ratio  $R_\mu(K_1)$  which comes through the different mixing angle  $\theta_{K_1} = -34^\circ, -45^\circ, -57^\circ$ , by draw the graph as a function of  $q^2$ . We find out that the ratio  $R_\mu(K_1)$  of final state meson  $K_1(1270)$  and  $K_1(1400)$ , is suitable for determining the  $K_1(1270) - K_1(1400)$  mixing angle,  $\theta_{K_1}$ . We have also summarized the numerical values of the branching fractions for  $K_1(1270)$  and  $K_1(1400)$ , corresponding to the different  $\theta_{K_1}$ . These analysis support the argument that this observable is suitable to fix the value of  $\theta_{K_1}$ . We also present our results for the longitudinal branching fraction  $R_\mu^L(K_1)$  and transverse branching fraction  $R_\mu^T(K_1)$ . These ratios are again show deviation at different  $\theta_{K_1}$ . The unpolarized  $R_\mu(K_1)$ , longitudinal  $R_\mu^L(K_1)$  and transverse  $R_\mu^T(K_1)$  ratios can be used to determine  $\theta_{K_1}$ .

**Table 4.3.** Input parameters for numerical calculations [59, 62, 65].

---



---

Mass and time of B meson,
$m_B = 5.279 \text{ GeV}, \tau_B = 1.54 \times 10^{-12} \text{ sec}$
Masses of Axial vector mesons in GeV,
$M_{K_1(1270)} = 1.272, M_{K_1(1400)} = 1.403, M_{K_{1A}} = 1.31, M_{K_{1B}} = 1.34$
CKM matrix elements,
$ V_{tb}V_{ts}^*  = 0.0407_{-0.0008}^{+0.0009}$
Mass of b quark,
$m_{b,\text{pole}} = 4.8 \pm 0.2$
Mass of muon,
$m_\mu = 0.105 \text{ GeV}.$
Guage coupling and fermi constant,
$\alpha_{EM} = \alpha = 1/137, G_F = 1.15 \times 10^{-5} \text{ GeV}^{-2}$

---

In the following tables we have mentioned the calculated numerical values of the observables  $\mathcal{BR}, \mathcal{A}_{FB}, f_L$  and  $R_\mu(K_1)$ , separately for  $B \rightarrow K_1(1270)\mu^+\mu^-$  and  $B \rightarrow K_1(1400)\mu^+\mu^-$  at different  $\theta_{K_1}$  and also in different  $q^2$  bins.

**Table 4.4.** Branching ratio  $\mathcal{BR}$  for  $B \rightarrow K_1(1270)\mu^+\mu^-$  at different angle in SM with negative and positive uncertainties in the form factors.

Mode	$\theta_{K_1}$	$\mathcal{BR} \times 10^{-6}$
$\mathcal{B}(B \rightarrow K_1(1270)\mu^+\mu^-)$	$-34^\circ$	$1.471_{-0.098}^{+0.284}$
	$-45^\circ$	$1.463_{-0.012}^{+0.155}$
	$-57^\circ$	$1.338_{-0.118}^{+0.004}$

**Table 4.5.** Branching ratio  $\mathcal{BR}$  for  $B \rightarrow K_1(1400)\mu^+\mu^-$  at different angle in SM with negative and positive uncertainties in the form factors.

Mode	$\theta_{K_1}$	$\mathcal{BR} \times 10^{-8}$
$\mathcal{B}(B \rightarrow K_1(1400)\mu^+\mu^-)$	$-34^\circ$	$3.812_{-0.565}^{+11.597}$
	$-45^\circ$	$3.725_{-8.047}^{+1.471}$
	$-57^\circ$	$12.813_{-10.338}^{+16.398}$

**Table 4.6.** Branching ratio for  $B \rightarrow K_1(1270)\mu^+\mu^-$  and  $B \rightarrow K_1(1400)\mu^+\mu^-$  in different bin of  $q^2$ .

Mode	$\theta_{K_1}$	[0.045 – 1]	[1 – 6]	[13 – max]
$\mathcal{B}(B \rightarrow K_1(1270)\mu^+\mu^-) \times 10^{-6}$	$-34^\circ$	0.161	0.086	0.071
	$-45^\circ$	0.167	0.082	0.073
	$-57^\circ$	0.160	0.072	0.069
$\mathcal{B}(B \rightarrow K_1(1400)\mu^+\mu^-) \times 10^{-8}$	$-34^\circ$	1.345	0.179	0.204
	$-45^\circ$	0.667	0.458	0.005
	$-57^\circ$	1.394	1.262	0.246

**Table 4.7.** Forward-backward symmetry for  $B \rightarrow K_1(1270)\mu^+\mu^-$  and  $B \rightarrow K_1(1400)\mu^+\mu^-$  in different bin of  $q^2$ .

Mode	$\theta_{K_1}$	[0.045 – 1]	[1 – 6]	[13 – max]
$A_{FB}(B \rightarrow K_1(1270)\mu^+\mu^-)$	$-34^\circ$	-0.107	0.220	0.259
	$-45^\circ$	-0.121	0.251	0.260
	$-57^\circ$	-0.137	0.291	0.262
$A_{FB}(B \rightarrow K_1(1400)\mu^+\mu^-)$	$-34^\circ$	-0.267	1.335	0.241
	$-45^\circ$	-0.017	0.016	-0.247
	$-57^\circ$	-0.010	0.032	0.217

**Table 4.8.** Helicity fraction for  $B \rightarrow K_1(1270)\mu^+\mu^-$  and  $B \rightarrow K_1(1400)\mu^+\mu^-$  in different bin of  $q^2$ .

Mode	$\theta_{K_1}$	[0.045 – 1]	[1 – 6]	[13 – max]
$f_L(B \rightarrow K_1(1270)\mu^+\mu^-)$	$-34^\circ$	0.671	0.798	0.404
	$-45^\circ$	0.639	0.775	0.399
	$-57^\circ$	0.603	0.747	0.393
$f_L(B \rightarrow K_1(1400)\mu^+\mu^-)$	$-34^\circ$	0.301	0.375	0.312
	$-45^\circ$	0.901	0.976	0.580
	$-57^\circ$	0.951	0.967	0.468

**Table 4.9.** Ratio  $R_\mu(K_1) = \mathcal{B}(B \rightarrow K_1(1400)\mu^+\mu^-)/(\mathcal{B}B \rightarrow K_1(1270)\mu^+\mu^-)$  in different bin of  $q^2$ .

Mode	$\theta_{K_1}$	[0.045 – 1]	[1 – 6]	[13 – max]
$R_\mu(K_1)$	$-34^\circ$	0.055	0.021	0.025
	$-45^\circ$	0.062	0.059	0.0005
	$-57^\circ$	0.164	0.185	0.030
$R_\mu^L(K_1)$	$-34^\circ$	0.031	0.009	0.017
	$-45^\circ$	0.094	0.071	0.001
	$-57^\circ$	0.258	0.235	0.037
$R_\mu^T(K_1)$	$-34^\circ$	0.096	0.075	0.030
	$-45^\circ$	0.012	0.008	0.0002
	$-57^\circ$	0.009	0.020	0.025

# Chapter 5

## Conclusion

We studied the semileptonic rare decay of B meson  $B \rightarrow K_1 \mu^+ \mu^-$  with  $K_1 \equiv K_1(1270)$ ,  $K_1(1400)$ . The strange axial-vector mesons,  $K_1(1270)$  and  $K_1(1400)$  are the mixtures of the  $K_{1A}$  and  $K_{1B}$ , which are the  $^3P_1$  and  $^1P_1$  states, respectively. We observed the branching ratio ( $\mathcal{BR}$ ), forward-backward asymmetry ( $\mathcal{A}_{FB}$ ), longitudinal helicity fraction ( $f_L$ ), ratio  $R_\mu(K_1) = \mathcal{B}(B \rightarrow K_1(1400) \mu^+ \mu^-) / \mathcal{B}(B \rightarrow K_1(1270) \mu^+ \mu^-)$ , longitudinal and transverse ratio ( $R_\mu^{(L,T)}(K_1)$ ) of final state meson  $K_1(1270)$  and  $K_1(1400)$  at different mixing angle  $\theta_{K_1} = -34^\circ, -45^\circ, -57^\circ$ .

We have calculated the  $\mathcal{BR}$  for  $K_1(1270)$  and  $K_1(1400)$  distinctively from our process  $B \rightarrow K_1(1270, 1400) \mu^+ \mu^-$ . It is observed that the  $\mathcal{BR}$  is suppressed for  $K_1(1400)$  as a final state meson compared to that of  $K_1(1270)$ . The physics is dominated by the  $\mathcal{O}_7$  operator in this region. At higher  $q^2$  values, there is an interference of the amplitudes controlled by the  $\mathcal{O}_9$  and  $\mathcal{O}_{10}$  operators, related to the loop. We observed from the plot that there are deviation in the distributions for the process  $B \rightarrow K_1(1400) \mu^+ \mu^-$  at different angle  $\theta_{K_1}$ , compare to the  $B \rightarrow K_1(1270) \mu^+ \mu^-$ .

We have found that the zero value of the  $\mathcal{A}_{FB}$  has not shown any change in case of  $B \rightarrow K_1(1270) \mu^+ \mu^-$  at three different angles  $\theta_{K_1}$ , but the zero value of  $\mathcal{A}_{FB}$  for process  $B \rightarrow K_1(1400) \mu^+ \mu^-$  show a shift at each  $\theta_{K_1}$  value, the shift in the zero position of  $\mathcal{A}_{FB}$  is towards low and higher  $q^2$  region for the angle  $-57^\circ$  and  $-45^\circ$  respectively, around the curve at  $\theta_{K_1} = -34^\circ$  whose zero position of  $\mathcal{A}_{FB}$  is at  $q^2 \simeq 3\text{GeV}^2$ .

We have also seen the longitudinal helicity fraction  $f_L$  for our desired process  $B \rightarrow K_1(1270, 1400)\mu^+\mu^-$ . It has been observed that the  $f_L$  for  $K_1(1270)$  meson is quite significant at low  $q^2$  region as we have seen the peak at low- $q^2$  region. The peak of the distribution of  $K_1(1270)$  is decreased at all  $q^2$  but shows no significant difference at different  $\theta_{K_1}$ . Where in case of  $K_1(1400)$  what we have seen that the  $f_L$  shows a large difference for different values of  $\theta_{K_1}$  at low- $q^2$  region.

We observed the variation in  $R_\mu(K_1) = \mathcal{B}(B \rightarrow K_1(1400)\mu^+\mu^-) / \mathcal{B}(B \rightarrow K_1(1270)\mu^+\mu^-)$  which comes through the different mixing angle  $\theta_{K_1} = -34^\circ, -45^\circ, -57^\circ$ , by drawing the graph as a function of  $q^2$ . We find out that the ratio  $R_\mu(K_1)$  of final state meson  $K_1(1270)$  and  $K_1(1400)$ , is suitable for determining the  $K_1(1270) - K_1(1400)$  mixing angle,  $\theta_{K_1}$ . We have also summarized the numerical values for  $K_1(1400)$  to  $K_1(1270)$  ratio, corresponding to the different  $\theta_{K_1}$ . These numerical analyses support the argument that this observable is suitable to fix the value of  $\theta_{K_1}$ . We also present our results for the longitudinal ratio  $R_\mu^L(K_1)$  and transverse ratio  $R_\mu^T(K_1)$ . These ratios again show deviation at different  $\theta_{K_1}$ . The unpolarized  $R_\mu(K_1)$ , longitudinal ratio  $R_\mu^L(K_1)$  and transverse ratio  $R_\mu^T(K_1)$  can be used to determine  $\theta_{K_1}$ .

Although the branching ratios depend on the magnitudes of  $B \rightarrow K_1$  form factors, the  $K_1(1270) - K_1(1400)$  mixing angle,  $\theta_{K_1}$ . The differential decay width with respect to the dilepton mass squared ( $d\Gamma/dq^2$ ),  $\mathcal{A}_{FB}$ ,  $f_L$  and  $R_\mu(K_1)$  have been measured by many experiments with no significant sign of deviations from the Standard Model expectation. All the above mentioned observables are sensitive for  $B \rightarrow K_1(1400)\mu^+\mu^-$  process as compared to the  $B \rightarrow K_1(1270)\mu^+\mu^-$  decay at different  $\theta_{K_1}$ . Hence the measurements of these observables at LHC, for the above mentioned processes can serve as a good tool to investigate the physics from the  $B \rightarrow K_1(1400)\mu^+\mu^-$ .

Particular in 2013 a local deviation of the observable from the standard model expectation was observed around GeV and then confirmed with larger data sets. Belle, ATLAS and CMS have subsequently presented data that are consistent with the LHCb results. This deviation triggered a lot of interest among theorists regarding B mesons.



# Bibliography

- [1] Gaillard, Mary K., Paul D. Grannis, and Frank J. Sciulli. "The standard model of particle physics." *Reviews of Modern Physics* 71, no. 2 (1999): S96.
- [2] Quigg, Chris. *Gauge theories of the strong, weak, and electromagnetic interactions*. Princeton University Press, 2013.
- [3] Delaere, Christophe. "Study of WW decay of a Higgs boson with the ALEPH and CMS detectors." PhD diss., Leuven U., 2005.
- [4] Herb, S. W., D. C. Hom, L. M. Lederman, J. C. Sens, H. D. Snyder, J. K. Yoh, J. A. Appel et al. "Observation of a dimuon resonance at 9.5 GeV in 400-GeV proton-nucleus collisions." *Physical Review Letters* 39, no. 5 (1977): 252.
- [5] Harrison, Paul F., and Helen R. Quinn. *The BaBar physics book: Physics at an asymmetric B factory*. No. SLAC-R-504. SLAC National Accelerator Lab., Menlo Park, CA (United States), 2010.
- [6] Abe, Kazuo, T. Abe, I. Adachi, H. Aihara, M. Akatsu, Y. Asano, T. Aso et al. "Improved measurement of mixing-induced CP violation in the neutral B meson system." *Physical Review D* 66, no. 7 (2002): 071102.
- [7] Kubota, Yuichi, J. K. Nelson, D. Perticone, R. Poling, S. Schrenk, M. S. Alam, Z. H. Bian et al. "The CLEO ii detector." *Nuclear Instruments and Methods in Physics Research Section A: Accelerators, Spectrometers, Detectors and Associated Equipment* 320, no. 1-2 (1992): 66-113.

- [8] Collaborations, S. L. D. "Combined results on b-hadron production rates, lifetimes, oscillations and semileptonic decays." arXiv preprint hep-ex/0009052 (2000).
- [9] F. Abe et al. [CDF Collaboration], Nucl. Instrum. Meth. A 271 (1988) 387; S. Abachi et al. [D0 Collaboration], Nucl. Instrum. Meth. A 338 (1994) 185
- [10] Glashow, Sheldon L., Jean Iliopoulos, and Luciano Maiani. "Weak interactions with lepton-hadron symmetry." Physical review D 2, no. 7 (1970): 1285.
- [11] Ammar, R., S. Ball, P. Baringer, Don Coppage, N. Coptly, R. Davis, N. Hancock et al. "Evidence for penguin-diagram decays: First observation of  $B \rightarrow K^*(892)\gamma$ ." Physical Review Letters 71, no. 5 (1993): 674.
- [12] Ali, Ahmed. "Rare B decays in the Standard Model." Nuclear Instruments and Methods in Physics Research Section A: Accelerators, Spectrometers, Detectors and Associated Equipment 384, no. 1 (1996): 8-16.
- [13] Buras, Andrzej J., and Manfred Münz. "Effective Hamiltonian for  $B \rightarrow X_s e^+ e^-$  beyond leading logarithms in the naive dimensional regularization and't Hooft-Veltman schemes." Physical Review D 52, no. 1 (1995): 186.
- [14] Ali, Ahmed, T. Mannel, and T. Morozumi. "Forward-backward asymmetry of dilepton angular distribution in the decay  $b \rightarrow sl^+l^-$ ." Physics Letters B 273, no. 4 (1991): 505-512.
- [15] S.R. Choudhury, N. Gaur, N. Mahajan, Phys. Rev. D 66, 054 003 (2002) [arXiv:hep-ph/0203041]; S.R. Choudhury, N. Gaur, arXiv:hep-ph/0205076; S.R. Choudhury, N. Gaur, arXiv:hep-ph/0207353.
- [16] U.O. Yilmaz, B.B. Sirvanli, G. Turan, Nucl. Phys. 692, 249 (2004) [arXiv:hep-ph/0407006]; U.O. Yilmaz, B.B. Sirvanli, G. Turan, Eur. Phys. J. C 30, 197 (2003) [arXiv:hep-ph/0304100].

- [17] Ali, A., E. Lunghi, C. Greub, and G. Hiller. "Improved model-independent analysis of semileptonic and radiative rare B decays." *Physical Review D* 66, no. 3 (2002): 034002.
- [18] C.H. Chen, C.Q. Geng, *Phys. Rev. D* 66, 034 006 (2002) [arXiv:hep-ph/0207038]; *Phys. Rev. D* 66, 014 007 (2002) [arXiv:hep-ph/0205306].
- [19] G. Erkol, G. Turan, *Nucl. Phys. B* 635, 286 (2002) [arXiv:hep-ph/0204219]; E.O. Iltan, G. Turan, I. Turan, *J. Phys. G* 28, 307 (2002) [arXiv:hep-ph/0106136].
- [20] W.J. Li, Y.B. Dai, C.S. Huang, arXiv:hep-ph/0410317.
- [21] Q.S. Yan, C.S. Huang, W. Liao, S.H. Zhu, *Phys. Rev. D* 62, 094 023 (2000) [arXiv:hep-ph/0004262].
- [22] S.R. Choudhury, N. Gaur, A.S. Cornell, G.C. Joshi, *Phys. Rev. D* 68, 054 016 (2003) [arXiv:hep-ph/0304084]; S.R. Choudhury, A.S. Cornell, N. Gaur, G.C. Joshi, *Phys. Rev. D* 69, 054 018 (2004) [arXiv:hep-ph/0307276].
- [23] F. Kruger, E. Lunghi, *Phys. Rev. D* 63, 014 013 (2001) [arXiv:hep-ph/0008210].
- [24] R. Mohanta, A.K. Giri, arXiv:hep-ph/0611068.
- [25] Roberts, W. "HQET and Form Factor Effects in  $B \rightarrow K^{(*)}\ell^+\ell^-$ ." arXiv preprint hep-ph/9512253 (1995).
- [26] Abe, K., R. Abe, I. Adachi, Byoung Sup Ahn, H. Aihara, M. Akatsu, Y. Asano et al. "Observation of the Decay  $B \rightarrow K l^+ l^-$ ." *Physical review letters* 88, no. 2 (2001): 021801.
- [27] Nardulli, G., and T. N. Pham. " $B \rightarrow K_1 \gamma$  and tests of factorization for two-body non-leptonic B decays with axial-vector mesons." *Physics Letters B* 623, no. 1-2 (2005): 65-72. 5

- [28] Yang, Heyoung, M. Nakao, K. Abe, H. Aihara, Y. Asano, T. Aushev, S. Bahinipati et al. "Observation of  $B^+ \rightarrow K_1^+(1270)\gamma$ ." *Physical review letters* 94, no. 11 (2005): 111802.
- [29] Abdesselam, A., I. Adachi, K. Adamczyk, H. Aihara, S. Al Said, K. Arinstein, Y. Arita et al. "Angular analysis of  $B^0 \rightarrow K^*(892)^0 \ell^+ \ell^-$ ." arXiv preprint arXiv:1604.04042 (2016).
- [30] Suzuki, Mahiko. "Strange axial-vector mesons." *Physical Review D* 47, no. 3 (1993): 1252.
- [31] Dutta, Rupak. "Model independent analysis of new physics effects on  $B_c \rightarrow (D_s, D_s^*)\mu^+\mu^-$  decay observables." *Physical Review D* 100, no. 7 (2019): 075025.
- [32] Hatanaka, Hisaki, and Kwei-Chou Yang. " $K_{1(1270)}-K_{1(1400)}$  mixing angle and new-physics effects in  $B \rightarrow K_1 l^+ l^-$  decays." *Physical Review D* 78, no. 7 (2008): 074007.
- [33] Peskin, Michael E., and Daniel V. Schroeder. "An Introduction to Quantum Field Theory Boulder, CO." (1995).
- [34] Pich, Antonio. "The Standard model of electroweak interactions." arXiv preprint arXiv:1201.0537 (2012).
- [35] Moore, Guy David. *The standard model: a primer*. Cambridge University Press, 2007.
- [36] Höcker, A., H. Lacker, S. Laplace, and F. Le Diberder. "A New approach to a global fit of the CKM matrix." *The European Physical Journal C-Particles and Fields* 21, no. 2 (2001): 225-259.
- [37] Amsler, Claude, Michael Doser, P. Bloch, A. Ceccucci, G. F. Giudice, A. Höcker, M. L. Mangano et al. "Review of particle physics." *Physics Letters B* 667, no. 1-5 (2008): 1-6.
- [38] Neubert, Matthias. "Effective field theory and heavy quark physics." In *Physics In D  $\geq$  4 Tasi 2004: TASI 2004*, pp. 149-194. 2006.

- [39] Polchinski, Joseph. "Effective field theory and the Fermi surface." arXiv preprint hep-th/9210046 (1992).
- [40] Höcker, A., H. Lacker, S. Laplace, and F. Le Diberder. "A New approach to a global fit of the CKM matrix." *The European Physical Journal C-Particles and Fields* 21, no. 2 (2001): 225-259.
- [41] Lee, Keith Seng Mun. "Effective field theories for inclusive B decays." PhD diss., Massachusetts Institute of Technology, 2006.
- [42] Nir, Yosef, and Dennis Silverman. "Z-mediated flavor-changing neutral currents and their implications for CP asymmetries in  $B^0$  decays." *Physical Review D* 42, no. 5 (1990): 1477..
- [43] Lowrey, Norman A. "Analysis of the neutral D-meson decay to a neutral kaon and two neutral pions." PhD diss., University of Illinois at Urbana-Champaign, 2010.
- [44] Ball, Patricia, and Vladimir M. Braun. "Exclusive semileptonic and rare B meson decays in QCD." *Physical Review D* 58, no. 9 (1998): 094016.
- [45] Buccella, Franco, Maurizio Lusignoli, Alessandra Pugliese, and Pietro Santorelli. "C P violation in D meson decays: Would it be a sign of new physics?." *Physical Review D* 88, no. 7 (2013): 074011.
- [46] Ali, Ahmed. "Flavour changing neutral current processes in B decays." *Nuclear Physics B-Proceedings Supplements* 59, no. 1-3 (1997): 86-100.
- [47] Buras, Andrzej J., and Robert Fleischer. "Quark mixing, CP violation and rare decays after the top quark discovery." *Advanced Series on Directions in High Energy Physics* 15 (1998): 65.
- [48] LHCb Collaboration. "Angular analysis of the  $B^0 \rightarrow K^{*0} \mu^+ \mu^-$  decay using 3 fb $^{-1}$  of integrated luminosity." *Journal of High Energy Physics* 2016, no. 2 (2016): 1-79.
- [49] Huang, Hsuan-Cheng. "Rare B decays at BELLE." Arxiv preprint hep-ex/0205062 (2002).

- [50] Ammar, R., S. Ball, P. Baringer, Don Coppage, N. Coptly, R. Davis, N. Hancock et al. "Evidence for penguin-diagram decays: First observation of  $B \rightarrow K^*(892)\gamma$ ." Physical Review Letters 71, no. 5 (1993): 674.
- [51] Beneke, Martin, Christoph Bobeth, and Robert Szafron. "Enhanced Electromagnetic Corrections to the Rare Decay  $B_{s,d} \rightarrow \mu^+\mu^-$ ." Physical review letters 120, no. 1 (2018): 011801.
- [52] Buras, Andrzej J. "Weak Hamiltonian, CP violation and rare decays." arXiv preprint hep-ph/9806471 (1998).
- [53] Buchalla, Gerhard, Andrzej J. Buras, and Markus E. Lautenbacher. "Weak decays beyond leading logarithms." Reviews of Modern Physics 68, no. 4 (1996): 1125.
- [54] Limosani, A., H. Aihara, K. Arinstein, T. Aushev, A. M. Bakich, V. Balagura, E. Barberio et al. "Measurement of inclusive radiative B-meson decays with a photon energy threshold of 1.7 GeV." Physical review letters 103, no. 24 (2009): 241801.
- [55] Greub, Christoph, Tobias Hurth, and Daniel Wyler. "Virtual corrections to the decay  $b \rightarrow s\gamma$ ." arXiv preprint hep-ph/9602281 (1996).
- [56] Lattice, Fermilab, M. I. L. C. Collaborations, Daping Du, A. X. El-Khadra, Steven Gottlieb, A. S. Kronfeld, J. Laiho, E. Lunghi, R. S. Van de Water, and Ran Zhou. "Phenomenology of semileptonic B-meson decays with form factors from lattice QCD." Physical Review D 93, no. 3 (2016): 034005.
- [57] Chen, Chuan-Hung, and Chao-Qiang Geng. "Baryonic rare decays of  $\Lambda_b \rightarrow \Lambda l^+l^-$ ." Physical Review D 64, no. 7 (2001): 074001.
- [58] Ali, Ahmed, Patricia Ball, L. T. Handoko, and G. Hiller. "Comparative study of the decays  $B \rightarrow (K, K^*)l^+l^-$  in the standard model and supersymmetric theories." Physical Review D 61, no. 7 (2000): 074024.

- [59] Tanabashi, Masaharu, K. Hagiwara, K. Hikasa, Katsumasa Nakamura, Y. Sumino, F. Takahashi, J. Tanaka et al. "Review of particle physics." *Physical Review D* 98, no. 3 (2018): 030001.
- [60] Yang, Kwei-Chou. "Form factors of  $B_{u,d,s}$  decays into p-wave axial-vector mesons in the light-cone sum rule approach." *Physical Review D* 78, no. 3 (2008): 034018.
- [61] P.Colangelo, F. De Fazio, R. Ferrandes, and T. N. Pham. "Spin effects in rare  $B \rightarrow X_s \tau^+ \tau^-$  and  $B \rightarrow K^{(*)} \tau^+ \tau^-$  decays in a single universal extra dimension scenario." *Physical Review D* 74, no. 11 (2006): 115006.
- [62] Yao, Wei-Ming, C. D. Amsler, David M. Asner, R. M. Barnett, J. Beringer, P. R. Burchat, C. D. Carone et al. "Review of particle physics." *Journal of Physics G: Nuclear and Particle Physics* 33, no. 1 (2006): 001.
- [63] Yang, Kwei-Chou. "Light-cone distribution amplitudes of axial-vector mesons." *Nuclear Physics B* 776, no. 1-2 (2007): 187-257.
- [64] Charles, Jérôme, O. Deschamps, S. Descotes-Genon, H. Lacker, A. Menzel, S. Monteil, V. Niess et al. "Current status of the standard model CKM fit and constraints on  $\Delta F = 2$  new physics." *Physical Review D* 91, no. 7 (2015): 073007.
- [65] Nakamura, K., C. Amsler, and Particle Data Group. "Particle physics booklet." *Journal of Physics G: Nuclear and Particle Physics* 37, no. 7A (2010): 075021.
- [66] Feldmann, Thorsten, and Joaquim Matias. "Forward-backward and isospin asymmetry for  $B \rightarrow K^* l^+ l^-$  decay in the standard model and in supersymmetry." *Journal of High Energy Physics* 2003, no. 01 (2003): 074.
- [67] Saddique, Asif, M. Jamil Aslam, and Cai-Dian Lü. "Lepton polarization asymmetry and forward-backward asymmetry in exclusive  $B \rightarrow K_1 \tau^+ \tau^-$  decay in universal extra dimension scenario." *The European Physical Journal C* 56, no. 2 (2008): 267-277.

- [68] Paracha, M. Ali, Ishtiaq Ahmed, and M. Jamil Aslam. "Semileptonic charmed B meson decays in universal extra dimension model." *Physical Review D* 84, no. 3 (2011): 035003.
- [69] Dai, Yuan-Ben, Chao-Shang Huang, and Han-Wen Huang. " $B \rightarrow X_s \tau^+ \tau^-$  in a two-Higgs doublet model." *Physics Letters B* 390, no. 1-4 (1997): 257-262.
- [70] Buras, Andrzej J., M. Misiak, M. Münz, and Stefan Pokorski. "Theoretical uncertainties and phenomenological aspects of  $b \rightarrow X_s \gamma$  decay." *Nuclear Physics B* 424, no. 2 (1994): 374-398.